CMS-HIG-17-008

arXiv:1806.00408v2 [hep-ex] 14 Dec 2018

Search for Higgs boson pair production in the $\gamma\gamma b\bar{b}$ final state in pp collisions at $\sqrt{s} = 13\,\text{TeV}$

The CMS Collaboration*

Abstract

A search is presented for the production of a pair of Higgs bosons, where one decays into two photons and the other one into a bottom quark-antiquark pair. The analysis is performed using proton-proton collision data at $\sqrt{s} = 13\,\text{TeV}$ recorded in 2016 by the CMS detector at the LHC, corresponding to an integrated luminosity of $35.9\,\text{fb}^{-1}$. The results are in agreement with standard model (SM) predictions. In a search for resonant production, upper limits are set on the cross section for new spin-0 or spin-2 particles. For the SM-like nonresonant production hypothesis, the data exclude a product of cross section and branching fraction larger than 2.0 fb at 95% confidence level (CL), corresponding to about 24 times the SM prediction. Values of the effective Higgs boson self-coupling κ_λ are constrained to be within the range $-11 < \kappa_\lambda < 17$ at 95% CL, assuming all other Higgs boson couplings are at their SM value. The constraints on κ_λ are the most restrictive to date.

*See Appendix A for the list of collaboration members

1 Introduction

The discovery of a particle with a mass of about 125 GeV, with properties compatible with those expected for the Higgs (H) boson of the standard model (SM) [1–3], has stimulated interest in the detailed exploration and understanding of the origin of the Brout–Englert–Higgs (BEH) mechanism [4, 5]. The production of a pair of Higgs bosons (HH) is a rare process that is sensitive to the structure of the BEH potential through the Higgs boson's self-coupling mechanism. In the SM, the corresponding production cross section via gluon-gluon fusion in proton-proton (pp) collisions at $\sqrt{s} = 13$ TeV is predicted to be $\sigma_{\text{gg}\to\text{HH}} = 33.5^{+2.5}_{-2.8}$ fb [6–8], a value beyond the reach of the analyses based on the current integrated luminosity of the CERN LHC program.

Many theories beyond the SM (BSM) suggest the existence of heavy particles that can couple to a pair of Higgs bosons. These particles could appear as a resonant contribution to the invariant mass of the HH system and induce a significant increase of the HH production cross section with respect to the SM. For example, models with warped extra dimensions (WED) [9] postulate the existence of compactified extra spatial dimensions. They predict new resonances decaying to a Higgs boson pair, including spin-0 radions R [10] and spin-2 Kaluza–Klein gravitons (KK graviton) [11]. The benchmark scenario considered in this paper, the bulk Randall–Sundrum (RS) model [12], assumes that all fields can propagate in the extra dimension. Models with an extended Higgs sector also predict a spin-0 resonance that decays to a pair of SM Higgs bosons, if sufficiently massive. Examples of such models are the singlet extension of the SM [13], the two-Higgs-doublet models [14] (in particular, the minimal supersymmetric model [15]), and the Georgi–Machacek model [16]. Many of these models predict that heavy scalar production occurs predominantly through the gluon-gluon fusion process. The Lorentz structure of the effective coupling between the scalar and the gluon is the same for a radion or a heavy Higgs boson. Therefore, the kinematics for the production of a radion or an additional Higgs boson are essentially the same, provided the spin-0 resonance is narrow. The radion results can therefore be applied to constrain this class of models.

If the new particles are too heavy to be observed through a direct search, they may contribute to HH production through virtual processes and lead to an enhancement of the cross section with respect to the SM prediction (as discussed, e.g., in Ref. [17]). In addition, different BSM models can modify the Higgs boson's fundamental couplings and impact HH production in gluon-gluon fusion [18] (ggHH) and vector boson fusion (VBF) [6, 8].

This letter describes a search for the production of pairs of Higgs bosons via $\text{pp} \to \text{HH} \to \gamma\gamma\text{b}\overline{\text{b}}$ using a data sample of 35.9 fb^{-1} collected by the CMS experiment in 2016. Both nonresonant and resonant production are explored, with the search for a narrow resonance X conducted at masses m_{X} between 260 and 900 GeV. The fully reconstructed $\gamma\gamma\text{b}\overline{\text{b}}$ final state combines the large SM branching fraction ($\mathcal{B}$) of the H $\to$ b$\overline{\text{b}}$ decay with the comparatively low background and good mass resolution of the H $\to \gamma\gamma$ channel, yielding a total $\mathcal{B}(\text{HH} \to \gamma\gamma\text{b}\overline{\text{b}})$ of 0.26% [6]. The search uses the mass spectra of the diphoton ($m_{\gamma\gamma}$), dijet (m_{jj}), and four-body systems ($m_{\gamma\gamma\text{jj}}$), as well as the associated helicity angles, to provide discrimination between the HH production signal and the other SM processes. The ggHH production process is studied in detail and the sensitivity of CMS data to the nonresonant VBF production mechanism is investigated for the first time.

Searches in the same and complementary final states such as HH $\to$ b$\overline{\text{b}}$b$\overline{\text{b}}$ or HH $\to \tau^+\tau^-$b$\overline{\text{b}}$ were performed in the past by the ATLAS [19–22] and CMS [23–28] Collaborations at $\sqrt{s} = 8$ and 13 TeV.

2 The CMS detector

The CMS detector, its coordinate system, and the main kinematic variables used in the analysis are described in detail in Ref. [29]. The central feature of the CMS apparatus is a superconducting solenoid, of 6 m internal diameter, providing a magnetic field of 3.8 T. A silicon pixel and strip tracker covering the pseudorapidity range $|\eta| < 2.5$, an electromagnetic calorimeter (ECAL) made of lead tungstate crystals, and a brass and scintillator hadron calorimeter reside within the field volume. Forward calorimeters extend the pseudorapidity coverage above $|\eta| = 3.0$. Muons are detected in gas-ionization chambers embedded in the steel flux-return yoke outside the solenoid. The first level of the CMS trigger system, composed of special hardware processors, uses information from the calorimeters and muon detectors to select the most interesting events in a time interval of less than $4\,\mu s$. The high-level trigger further decreases the event rate, from around 100 kHz to less than 1 kHz, before data storage [30].

3 Simulated events

Signal samples are simulated at leading order (LO) using MADGRAPH5_aMC@NLO 2.3.2 [31–33] interfaced with LHAPDF6 [34]. The next-to-leading-order (NLO) parton distribution function (PDF) set PDF4LHC15_NLO_MC is used [35–39]. The models describe the production through gluon-gluon fusion of particles with narrow width (set to 1 MeV) that decay to two Higgs bosons with the mass of $m_H = 125$ GeV [40]. Events are generated either for spin-0 radion production, or spin-2 KK graviton production, as predicted by the bulk RS model. For each spin hypothesis 16 mass points are generated within the range $260 \leq m_X \leq 900$ GeV in steps of 10 GeV for m_X between 260 and 300 GeV, and in steps of 50 GeV for m_X above 300 GeV.

In the nonresonant case we use the effective field theory approach and notations from Refs. [6, 41]. First we consider two SM coupling modifiers: $\kappa_\lambda \equiv \lambda_{HHH}/\lambda_{HHH}^{SM}$, which measures deviations of the Higgs boson trilinear coupling λ_{HHH} from its SM expectation, $\lambda_{HHH}^{SM} \equiv m_H^2/(2v^2) = 0.129$; and $\kappa_t \equiv y_t/y_t^{SM}$, which measures deviations of the top quark Yukawa coupling y_t from its SM expectation $y_t^{SM} = \sqrt{2}\,m_t/v \approx 1.0$. Here $v = 246$ GeV denotes the vacuum expectation value of the Higgs boson, m_H its mass, and m_t denotes the top quark mass. Second, we also consider couplings not found in the SM that are derived from dimension-6 operators: contact interactions between two Higgs bosons and two top quarks (c_2), between one Higgs boson and two gluons (c_g), and between two Higgs bosons and two gluons (c_{2g}). We define these three parameters in such a way that their values are zero within the SM. The most general production is described by a modification of the SM Lagrangian, the relevant part of which, labelled as $\mathcal{L}_{HH}$, is given in the following equation [42]:

$$\mathcal{L}_{HH} = \kappa_\lambda \lambda_{HHH}^{SM} v H^3 - \frac{m_t}{v}\left(\kappa_t H + \frac{c_2}{v} H^2\right)\left(\bar{t}_L t_R + \text{h.c.}\right) + \frac{1}{4}\frac{\alpha_S}{3\pi v}\left(c_g H - \frac{c_{2g}}{2v} H^2\right) G^{\mu\nu} G_{\mu\nu}, \quad (1)$$

where t_L and t_R are the top quark fields with left and right chiralities, respectively. The H denotes the physical Higgs boson field, $G^{\mu\nu}$ is the gluon field strength tensor, and α_S is the strong coupling constant. The notation $h.c.$ is used for the Hermitian conjugate. Five main Feynman diagrams, shown in Fig. 1, contribute to ggHH at LO.

The cross section is expressed at LO as a function of five BSM parameters (κ_λ, κ_t, c_2, c_g, and c_{2g}) [6, 41] and this parametrization is approximately extended to the next-to-next-to-leading order matched to the next-to-next-to-leading log in quantum chromodynamics (QCD) using a global k-factor [6, 7, 43] that has uncertainties coming from the PDF, missing orders, α_S and finite top quark mass effects. There is a dependence of the k-factors on m_{HH} related to the finite
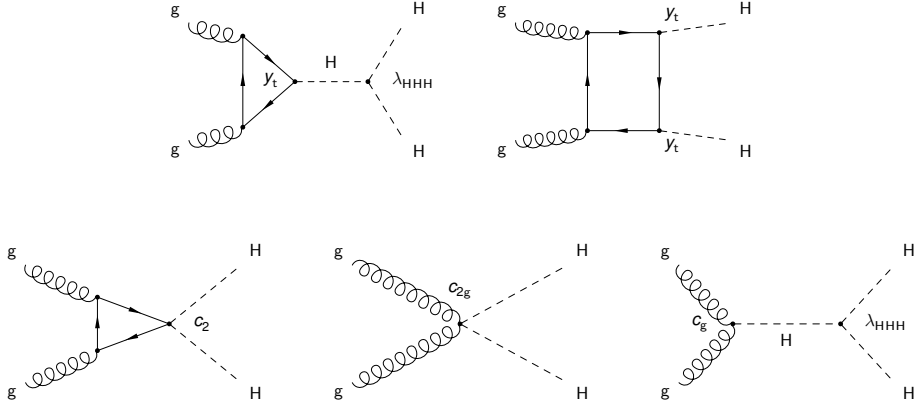
Figure 1: Feynman diagrams that contribute to ggHH at LO. Top diagrams correspond to SM-like processes, referred to as box and triangle diagrams, respectively. The bottom diagrams correspond to pure BSM processes: the first exploits the contact interaction of two Higgs bosons with two top quarks and the last two describe contact interactions between the H boson and gluons.

top quark mass effects [44]. Within the region of sensitivity of this analysis, $m_{HH} < 900\,\text{GeV}$, any effect is covered by the total k-factor uncertainty. The departure of the parameters from their SM values can change the total cross section by a few orders of magnitude. Furthermore, the kinematic properties of the HH final state are modified, which affects the final sensitivity through the modification of the acceptance and efficiency of the experimental analysis.

To avoid a prohibitively large number of samples to simulate and to analyze, we use the method proposed in Refs. [6, 41, 45] to partition the parameter space into 12 regions with distinct kinematics, referred to as clusters. Each of the clusters with its HH kinematics can be represented by a point in the 5D parameter space that is referred to as a *benchmark hypothesis*. We simulate the 12 benchmark hypotheses together with two additional ones – one assuming all parameters to be SM ones (referred to as *SM benchmark hypothesis*) and the other using identical assumptions except for a vanishing Higgs boson self-coupling (referred to as $\kappa_\lambda = 0$). The list of benchmark hypotheses is provided in Table 1. An additional HH sample is produced via the VBF mechanism using SM couplings.

The ensemble of events obtained by combining all 14 gluon-gluon initiated samples covers the possible kinematic configurations of the effective field theory parameter space. These events can therefore subsequently be reweighted using the procedure derived in Ref. [46] to model any desired point in the full 5D parameter space. In this procedure, an event-by-event weight is analytically calculated from the generator-level information on the HH system.

Table 1: Parameter values of nonresonant BSM benchmark hypotheses. The first two columns correspond to the SM and $\kappa_\lambda = 0$ samples, respectively, while the next 12 correspond to the benchmark hypotheses identified using the method from Ref. [45].

	SM	$\kappa_\lambda = 0$	1	2	3	4	5	6	7	8	9	10	11	12
κ_λ	1.0	0.0	7.5	1.0	1.0	−3.5	1.0	2.4	5.0	15.0	1.0	10.0	2.4	15.0
κ_t	1.0	1.0	1.0	1.0	1.0	1.5	1.0	1.0	1.0	1.0	1.0	1.5	1.0	1.0
c_2	0.0	0.0	−1.0	0.5	−1.5	−3.0	0.0	0.0	0.0	0.0	1.0	−1.0	0.0	1.0
c_g	0.0	0.0	0.0	−0.8	0.0	0.0	0.8	0.2	0.2	−1.0	−0.6	0.0	1.0	0.0
c_{2g}	0.0	0.0	0.0	0.6	−0.8	0.0	−1.0	−0.2	−0.2	1.0	0.6	0.0	−1.0	0.0

The dominant backgrounds to the $\gamma\gamma b\bar{b}$ final state are those in which two objects identified as photons (either prompt photons or jets misidentified as photons) are produced in association with jets (referred to as $n\gamma + $ jets). The simulation of these final states is challenging due to large effects from higher orders in QCD [47] and limited knowledge of fragmentation effects in the case of a jet misidentified as a photon. In this analysis, these contributions are modeled entirely from data.

Single Higgs boson production in the SM, with two additional jets and with a subsequent decay of the Higgs boson to two photons, is also considered. In some cases, additional jets can be effectively initiated by b quarks, but in others they can be initiated by lighter quarks and misidentified as a b jet. The considered processes — gluon-gluon fusion (ggH), VBF, and associated production with $t\bar{t}$ (ttH), $b\bar{b}$ (b$\bar{b}$H), and vector bosons (VH) — are sources of background in this analysis. They are simulated using MADGRAPH5_aMC@NLO 2.2.2 for VH and 2.3.3 for b$\bar{b}$H, and POWHEG 2.0 [48–51] at NLO for ggH, VBF H , and $t\bar{t}$H. All single-Higgs background samples are normalized to the SM cross section as recommended in Ref. [6].

All generated events are processed with PYTHIA 8.212 [52] with the tune CUETP8M1 [53] for showering, hadronization, and the underlying event description, and GEANT4 [54] for the simulation of the CMS detector response. The simulated events include multiple overlapping pp interactions occurring in the same bunch crossing (pileup) as observed in the data.

4 Data set and event selection

Events are selected using double-photon triggers, which require two photons with transverse momenta $p_T^{\gamma 1} > 30\,\text{GeV}$ and $p_T^{\gamma 2} > 18\,\text{GeV}$ for the leading and subleading photons, respectively. In addition, calorimeter-based isolation and shower shape requirements are imposed online on the two photons. Finally, the diphoton invariant mass is required to exceed 90 GeV.

In the offline selection, events are required to have at least one well-identified pp collision vertex with a position less than 24 cm away from the nominal interaction point in the z-direction. The primary vertex is identified by a multivariate analysis that was trained for the measurement of $H \rightarrow \gamma\gamma$ production [55]. This analysis uses the momenta of the charged particle tracks associated with the vertex, and variables that quantify the vector and scalar balance of p_T between the diphoton system and the charged particle tracks associated with the vertex. The presence of at least two jets in the final state of this analysis helps to correctly identify the primary vertex in more than 99.9% of the simulated signal events.

4.1 The $H \rightarrow \gamma\gamma$ candidate

Photons are identified using a multivariate technique that includes as inputs the p_T of the electromagnetic shower, its longitudinal leakage into the hadron calorimeter, and its isolation from jet activity in the event. It was designed during the data taking at $\sqrt{s} = 8\,\text{TeV}$ [55, 56] and retrained with $\sqrt{s} = 13\,\text{TeV}$ data. Identified photon candidates with a track matched to the ECAL cluster are rejected. Photon energies are calibrated subsequently and their energies in simulated samples are smeared to match the resolution in data [55].

Events are required to have at least two identified photon candidates that are within the ECAL and tracker fiducial region ($|\eta| < 2.5$), but excluding the ECAL barrel-endcap transition region ($1.44 < |\eta| < 1.57$). The photon candidates are required to pass the following criteria: $100 < m_{\gamma\gamma} < 180\,\text{GeV}$; $p_T^{\gamma 1}/m_{\gamma\gamma} > 1/3$ and $p_T^{\gamma 2}/m_{\gamma\gamma} > 1/4$. In cases where more than two photons are found, the photon pair with the highest transverse momentum $p_T^{\gamma\gamma}$ is chosen.

For events that pass the above selections, the trigger efficiency is measured to be close to 100% using data events containing a Z boson decaying to a pair of electrons, or to a pair of electrons or muons in association with a photon [56].

4.2 The H $\to$ b$\bar{\text{b}}$ candidate

The particle-flow (PF) algorithm aims to reconstruct each individual particle (referred to as a PF candidate) in an event with an optimized combination of information from the various elements of the CMS detector [57]. Jets are clustered from these candidates using the anti-k_T algorithm with a distance parameter $R_j = 0.4$ [58, 59]. Jet candidates are required to have $p_T > 25$ GeV and $|\eta| < 2.4$. In addition, identification criteria are applied to remove spurious jets associated with calorimeter noise. Finally, jets must be separated from each of the two selected photon candidates by a distance $\Delta R_{\gamma j} \equiv \sqrt{(\Delta\eta_{\gamma j})^2 + (\Delta\phi_{\gamma j})^2} > 0.4$, where ϕ is the azimuthal angle in radians. The selected jets are combined into dijet candidates. At least one dijet candidate is necessary for an event to be selected. The combined secondary vertex algorithm, optimized for 13 TeV data, provides a continuous b tagging score defined between 0 and 1. It is used to quantify the probability that a jet is a result of a b quark hadronization [60]. In cases where more than two jets are found, the dijet constructed from the two jets with the highest b tagging scores is selected. An event is accepted if $70 < m_{jj} < 190$ GeV.

The energies of the two selected jets are corrected using the standard CMS algorithm, which is flavor blind [61]. In addition to this correction, a jet energy regression procedure is used to improve the m_{jj} resolution. A multivariate analysis technique is used to correct the absolute scale of the heavy-quark jets by taking into account their specific fragmentation features, i.e., a larger contribution from charged leptons and neutrinos than in light-quark jets. The approach we use in this letter is similar to the one used in the CMS search for the SM H $\to$ b$\bar{\text{b}}$ decays [62], and in addition, takes advantage of variables related to the missing transverse momentum vector, $\vec{p}_T^{\text{miss}}$, to estimate the neutrino contribution to the heavy-quark decay. The $\vec{p}_T^{\text{miss}}$ is calculated as the negative of the vectorial sum of the transverse momenta of all PF candidates. The jets forming the dijet candidate are ordered by p_T, and an optimized energy regression distinguishes the higher p_T jet from the lower p_T one. The improvement to the m_{jj} resolution due to the regression procedure depends on the b jet p_T spectrum characteristic of a given signal hypothesis. For example, for the SM-like search it is of the order of 15%.

4.3 The HH system

A summary of the baseline selection requirements is presented in Table 2. After the diphoton and dijet candidates are selected, they are combined to form an HH candidate.

Table 2: Summary of the baseline selection criteria.

Photons		Jets	
Variable	Selection	Variable	Selection
$p_T^{\gamma 1}$	$>m_{\gamma\gamma}/3$	p_T [GeV]	>25
$p_T^{\gamma 2}$	$>m_{\gamma\gamma}/4$	$\Delta R_{\gamma j}$	>0.4
$|\eta|$	<2.5	$|\eta|$	<2.4
$m_{\gamma\gamma}$ [GeV]	$[100, 180]$	m_{jj} [GeV]	$[70, 190]$

To have a better estimate of m_{HH} we correct $m_{\gamma\gamma jj}$ using

$$\widetilde{M}_X = m_{\gamma\gamma jj} - (m_{jj} - m_H) - (m_{\gamma\gamma} - m_H), \qquad (2)$$

which mitigates the $m_{\gamma\gamma jj}$ dependency on the dijet and diphoton energy resolutions with the assumption that the dijet and diphoton originate from a Higgs boson decay [63]. This procedure has an effect similar to the kinematic fit used previously in Ref. [23]. While for the distance parameter $R_j = 0.5$ used in Ref. [23] the kinematic fit was the best option to reconstruct m_{HH}, for the smaller radius used in this paper $\widetilde{M}_X$ appears to be more efficient. The improvements in the m_{HH} reconstruction are most striking for low-m_X hypotheses, as shown in Fig. 2, and have little impact on high m_X hypotheses. This effect can be understood by the fact that the relative contribution to $\widetilde{M}_X$ of $|m_{jj} - m_H|$ is much smaller at high m_X.
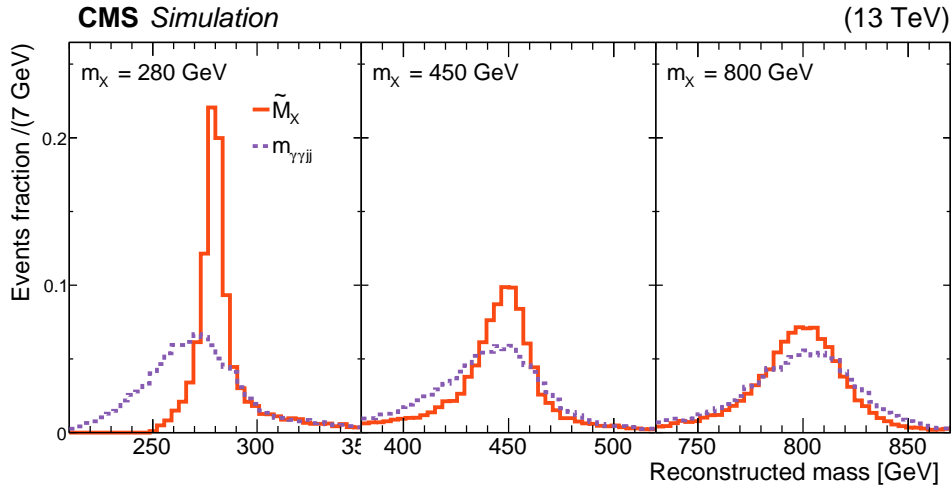
Figure 2: Comparison of $\widetilde{M}_X$ (red line) with $m_{\gamma\gamma jj}$ (purple dotted line) for different spin-2 resonance masses. All distributions are obtained after the full baseline selection (Table 2), and are normalized to unit area.

With the four reconstructed objects from the HH decay, angular correlations in the signal can provide important information to separate it from the background. In this analysis we consider three helicity angles. The scattering angle, θ_{HH}^{CS}, is defined in the Collins–Soper (CS) frame of the four-body system [64], as the angle between the momentum of the Higgs boson decaying into two photons and the line that bisects the acute angle between the colliding protons. Since the directions of the two Higgs boson candidates are collinear in the CS frame, the choice of the Higgs boson decaying to photons as the reference direction is arbitrary. Therefore, we use the absolute value of the cosine of this angle $|\cos\theta_{HH}^{CS}|$ to obviate this arbitrariness. The H boson decay angles are defined, in a way similar to Ref. [64], as the angles of the decay products in each Higgs boson's rest frame with respect to the direction of motion of the boson in the CS frame. Since the two photons from the Higgs boson decay are indistinguishable and the charges of the b quarks are not considered in this analysis, the absolute values of the cosines of these angles are used: $|\cos\theta_{\gamma\gamma}|$ and $|\cos\theta_{jj}|$.

4.4 Background properties

The main kinematic distributions of the $\gamma\gamma b\bar{b}$ final state that are used throughout the analysis (invariant masses and helicity angles) are shown in Fig. 3, after the basic selections summarized in Table 2. The data in Fig. 3 are dominated by $n\gamma$ + jets events, which are the primary contribution to the background in this region of phase space. The SM single-Higgs boson production processes, represented by colored areas in the figure, are three orders of magnitude lower than the nonresonant $n\gamma$ + jets processes. Only single-Higgs boson production processes with a sufficient number of events (t$\bar{\text{t}}$H, VH, and ggH) are shown for clarity of the figure. Finally, sig-
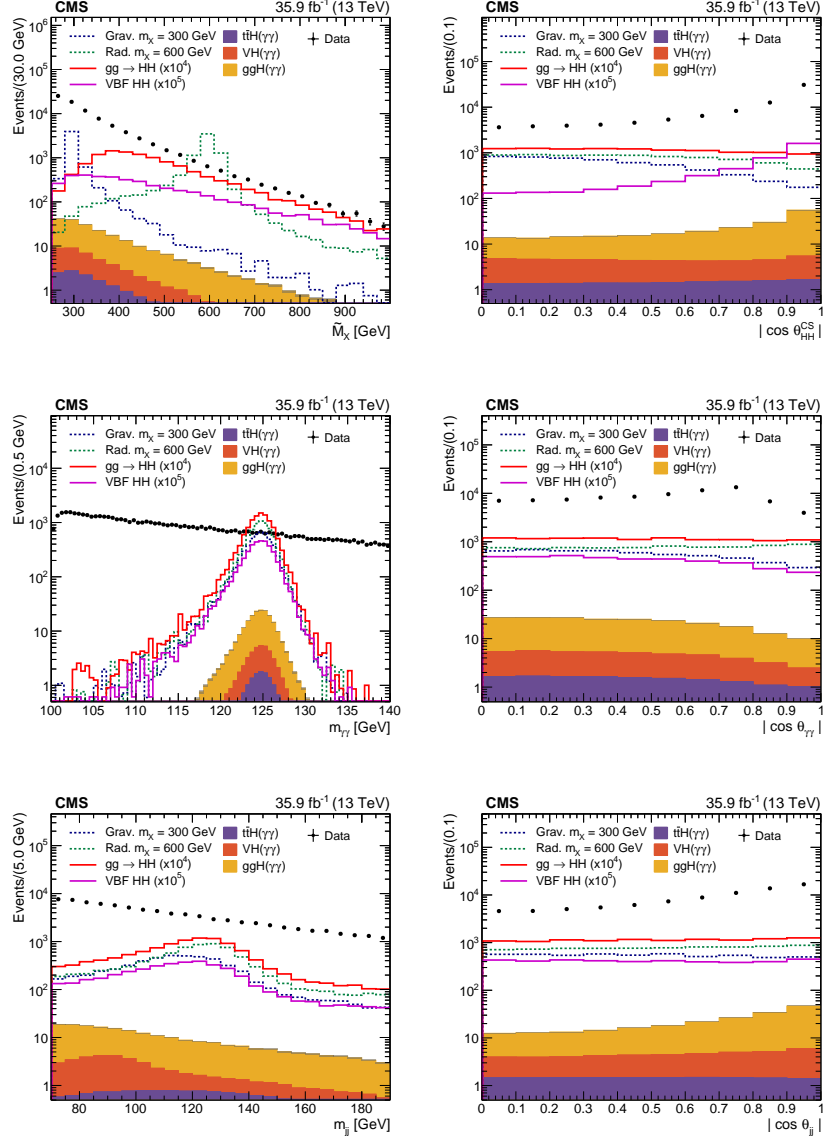
Figure 3: Data (dots), dominated by $n\gamma$ + jets background, compared to different signal hypotheses and three single-Higgs boson samples ($t\bar{t}$H, VH, and ggH) after the selections on photons and jets summarized in Table 2 for the kinematic distributions described in Sections 1 and 4.3: $\widetilde{M}_X$ (top left) and $|\cos\theta_{HH}^{CS}|$ (top right); $m_{\gamma\gamma}$ (middle left) and $|\cos\theta_{\gamma\gamma}|$ (middle right); m_{jj} (bottom left) and $|\cos\theta_{jj}|$ (bottom right). The statistical uncertainties on the data are barely visible beyond the markers. The resonant signal cross section is normalized to 500 fb and the SM-like ggHH (VBF HH) process to 10^4 (10^5) times its cross section.

nal shapes are shown in the figures, where the resonant ones have been normalized to a cross section of 500 fb and the SM-like ggHH (VBF HH) signal to 10^4 (10^5) times its cross section.

As expected, the signals produce peaks in $m_{\gamma\gamma}$ and m_{jj}. The resonant di-Higgs boson signals peak sharply in $\widetilde{M}_X$, while SM HH processes exhibit broad structures induced by the interference pattern of different Feynman diagrams contributing to the HH production and shaped by the analysis selections. The data show a smoothly falling mass spectrum, as expected for the $n\gamma$ + jets background. Finally, the single-Higgs boson backgrounds peak in $m_{\gamma\gamma}$, but not in m_{jj} or $\widetilde{M}_X$ (except the VH process which gives a peak in m_{jj} around the V masses).

The $|\cos\theta_{\mathrm{HH}}^{\mathrm{CS}}|$ distribution is sensitive to the tensor structure of the production mechanism (see for example Ref. [65]). It is relatively flat for ggHH [66] and the spin-0 mediated production. For the spin-2 mediated production it decreases toward 1, while for VBF HH and the data it rises toward 1. The distribution of the cosine of the H $\rightarrow \gamma\gamma$ helicity angle is expected to be flat for the samples with genuine Higgs bosons. The decrease toward 1 is due to the selections on photon p_{T}. In the data the distribution rises up to 0.8 and then decreases. This shape results from the combination of matrix element properties and the asymmetric selections on the photon p_{T}. In the same way, the $|\cos\theta_{\mathrm{jj}}|$ distribution is flat for the signal, but rises significantly toward 1 for the data and ggH.

5 Event classification and modeling

After dijet and diphoton candidate selection, events are placed into categories using the $\widetilde{M}_{\mathrm{X}}$ variable and a multivariate (MVA) classifier. Both variables are designed to minimize the correlation between $m_{\gamma\gamma}$ and m_{jj}. In each category, a parametric fit is performed in the two-dimensional $m_{\gamma\gamma} - m_{\mathrm{jj}}$ plane for the signal extraction procedure using a product of probability densities (PDs) for signal and backgrounds. This 2D approach helps to constrain the impact of the single-Higgs boson background since its structure in m_{jj} differs from that of the signal. Finally, all the categories are combined together assuming a signal model to maximize the sensitivity of the analysis.

5.1 Event classification

5.1.1 $\widetilde{M}_{\mathrm{X}}$ categorization

In the nonresonant search, a categorization is performed using the $\widetilde{M}_{\mathrm{X}}$ information. Since the $\widetilde{M}_{\mathrm{X}}$ spectrum for SM-like ggHH production has a maximum at around 400 GeV and the $n\gamma + $ jets background peaks at the kinematic threshold of $250\,\mathrm{GeV} = 2m_{\mathrm{H}}$, the maximal sensitivity is achieved for $\widetilde{M}_{\mathrm{X}} > 350\,\mathrm{GeV}$. However, anomalous couplings may change the $\widetilde{M}_{\mathrm{X}}$ distribution for the signal hypothesis. Therefore, instead of imposing a $\widetilde{M}_{\mathrm{X}}$ selection, events are categorized in the nonresonant search into high-mass (HM) and low-mass (LM) regions that are above and below $\widetilde{M}_{\mathrm{X}} = 350\,\mathrm{GeV}$, respectively.

In the resonant search, $\widetilde{M}_{\mathrm{X}}$ is used to define a unique signal region that depends on the mass of the resonance being sought. This mass window typically contains 60% of the signal at low m_{X}, increasing gradually for higher m_{X}. The resonant search starts just above the threshold at $260\,\mathrm{GeV} \gtrsim 2m_{\mathrm{H}}$ and extends up to $m_{\mathrm{X}} = 900\,\mathrm{GeV}$. In fact the R_{j} value used in this paper is small enough to reconstruct the decay products of two boosted b quarks produced in the Higgs boson decays as separate jets up to $m_{\mathrm{X}} \approx 1.25\,\mathrm{TeV}$ [67]. However, for values of $m_{\mathrm{X}} \approx 1\,\mathrm{TeV}$ and larger the available amount of data is too small to perform the signal extraction procedure as defined in this paper.

5.1.2 MVA categorization

An MVA procedure is used to select the most signal-like events and to further classify them. With this goal, a boosted decision tree (BDT) is trained with the TMVA package [68] using three types of variables:

- b tagging variables: the b tagging score of each jet in the dijet candidate;
- Helicity angles as defined in Section 4.3;

- HH transverse balance variables: $p_T^{\gamma\gamma}/m_{\gamma\gamma jj}$ and $p_T^{jj}/m_{\gamma\gamma jj}$, where p_T^{jj} is the transverse momentum of the dijet candidate.

The BDT is trained with the ensemble of ggHH samples as the signal hypothesis in the non-resonant search separately for low- and high-mass categories. For the resonant cases, the ensemble of resonant signals is used to train one BDT for $m_X < 600\,\text{GeV}$ and another one for $m_X > 600\,\text{GeV}$. This training strategy maximizes the sensitivity to massive resonances. The background events used for the training are obtained from a control sample that was extracted from the data by inverting the identification condition on one of the two photons. This sample is dominated by events having a photon produced with three accompanying jets. We verified that after excluding the events with $120 < m_{\gamma\gamma} < 130\,\text{GeV}$ in the signal and control samples, the kinematic properties of these two samples are well matched.
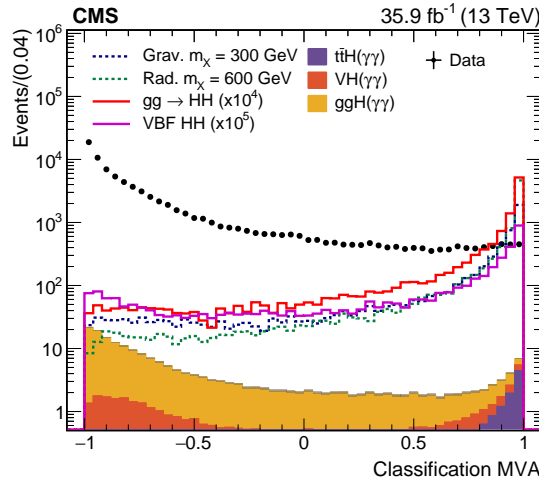
Figure 4: Distributions of the BDT output (classification MVA) obtained for the high-mass non-resonant training. Data, dominated by $n\gamma + \text{jets}$ background, are compared to different signal hypotheses and three single-Higgs boson samples (t$\bar{\text{t}}$H, VH, and ggH) after the selections on photons and jets summarized in Table 2. The statistical uncertainties on the data are barely visible beyond the markers. The resonant signal cross section is normalized to $500\,\text{fb}$ and the SM-like ggHH (VBF HH) process to 10^4 (10^5) times its cross section.

Figure 4 shows the BDT output from one of the four trainings. The MVA efficiently separates gluon-gluon produced signals from the $n\gamma + \text{jets}$ background that represents the dominant contribution to the data. The most powerful discriminating variables used in the BDT are the b tagging scores of the jets, followed by the kinematic variables. Therefore, the single-Higgs boson production samples with genuine contributions from two b quarks (t$\bar{\text{t}}$H and $Z(\to b\bar{b})H$) are classified as more signal-like, while ggH and other VH processes are classified as more background-like. Finally, events from the VBF HH production are selected less efficiently than those from ggHH production.

For a given category the purity is defined as the ratio between the number of events coming from a hypothetical signal with a production cross section normalized to 1 fb and the number of background events. For each of the four trainings, the output of the MVA classifier is used to define a category with the highest purity (HPC) and another with medium purity (MPC). The remaining events are rejected, because they do not improve the sensitivity of the analysis. In the nonresonant low-$\widetilde{M}_X$ MPC region, an additional requirement is placed on the b tagging score, corresponding to 80% efficiency for genuine b jets [60]. This reduces the contribution of the events where the jet with lowest b tagging score comes from a pileup event. Table 3

Table 3: Definition of high-purity category (HPC) and medium-purity category (MPC) for the resonant and nonresonant analyses.

Analysis	Region	Classification MVA	$\widetilde{M}_X$
Nonresonant	High-mass	HPC: MVA > 0.97 MPC: 0.6 < MVA < 0.97	$\widetilde{M}_X > 350\,\text{GeV}$
	Low-mass	HPC: MVA > 0.985 MPC: 0.6 < MVA < 0.985	$\widetilde{M}_X < 350\,\text{GeV}$
Resonant	$m_X > 600\,\text{GeV}$	HPC: MVA > 0.5 MPC: 0 < MVA < 0.5	Mass window
	$m_X < 600\,\text{GeV}$	HPC: MVA > 0.96 MPC: 0.7 < MVA < 0.96	Mass window

shows the HPC and MPC definitions for the different regions of the resonant and nonresonant analyses.

5.1.3   Signal acceptance times efficiency

The typical signal acceptance times efficiency ($A\epsilon$) values obtained in the resonant analysis are shown in Fig. 5. Consecutive effects of the selections on $A\epsilon$ for different analysis steps are shown: after the trigger selection that includes a loose online preselection on the photons, after the diphoton candidate selection, after the dijet candidate selection, and after the MVA categorization. The final $A\epsilon$ values range from approximately 20% (low mass) to 50% (high mass) for both the spin-0 and spin-2 resonance hypotheses. For an identical m_X value, $A\epsilon$ is a bit higher for a spin-2 hypothesis than for spin-0, because the Higgs bosons are, on average, produced more centrally in the KK graviton model considered in this letter (see Fig. 3).

The $A\epsilon$ value is 30 (13)% for the SM-like ggHH (VBF HH) signal hypothesis, with 25 (10)% in the high-mass region and 5 (3)% in the low-mass one. The difference between the two production mechanisms mainly comes from the fact that the MVA was trained assuming a ggHH signal. For example, one of the most discriminating variables, $|\cos\theta_{HH}^{CS}|$, shown in Fig. 3, has a similar behavior to the $n\gamma$ + jets background and for the VBF HH process, while it is very different for the ggHH process.

5.2   Signal modeling

The signal PD of each mass dimension is modeled with a double-sided Crystal Ball (CB) function, which is a modified version of the standard CB function [69] with two independent exponential tails. This modeling is useful in situations in which a lower-energy tail might be created by energy mismeasurements and a higher-energy tail by the mismatching of objects (for example when a jet from additional QCD radiation is misidentified as one of the jets from the H boson decay). The final two-dimensional signal model PD is the product of the independent $m_{\gamma\gamma}$ and m_{jj} models. The no-correlation hypothesis is checked by comparing the two-dimensional $m_{\gamma\gamma} - m_{jj}$ distribution from the simulated signal samples with the two-dimensional PD built as a product of one-dimensional ones. For the typical expected number of signal events in this analysis, the impact of such correlations is found to be negligible.

The PD parameters are obtained by fitting the simulated signal samples in each analysis region. For each m_X point and each nonresonant sample a dedicated fit is performed. The resolution is estimated by the σ_{eff} value, defined as half of the width of the narrowest region containing 68.3% of the signal shape. Examples of the signal shapes in the nonresonant analysis, assuming an SM-like signal, are shown in Fig. 6. The diphoton resolution is determined to be $\approx 1.6\,\text{GeV}$
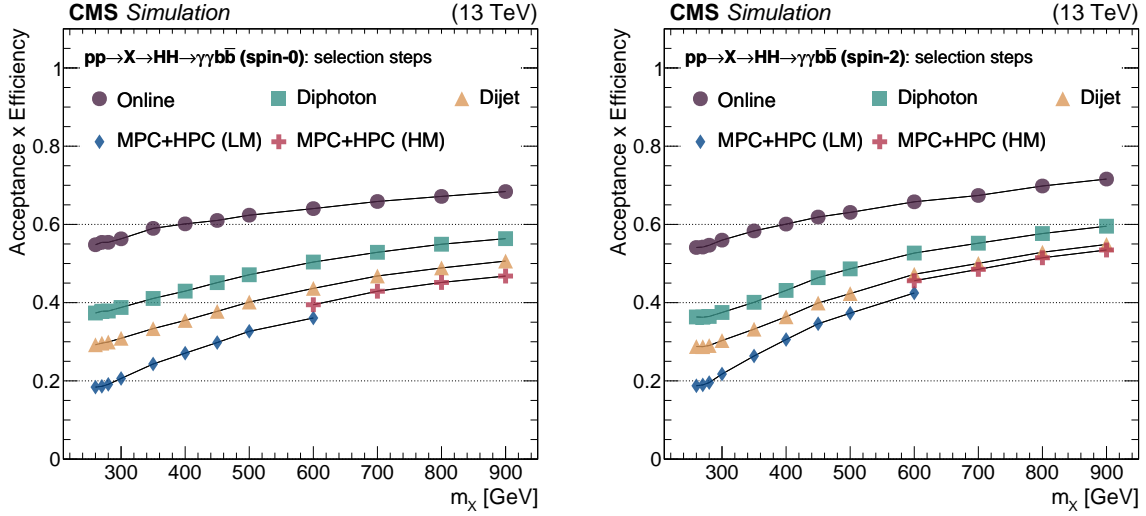
Figure 5: Consecutive selection efficiencies for different analysis steps for two resonance hypotheses: spin-0 (left) and spin-2 (right). Online selection includes the photon online preselection conditions described at the beginning of Section 4. Diphoton selections include photon identification and kinematics selections from Table 2. Dijet selections are those described in Table 2.

and the dijet resolution is $\approx 20\,\text{GeV}$. The mean of the Gaussian core of the CB function, μ, is close to m_{H}, within 0.1-0.2% for $m_{\gamma\gamma}$ and 1-2% for m_{jj}.
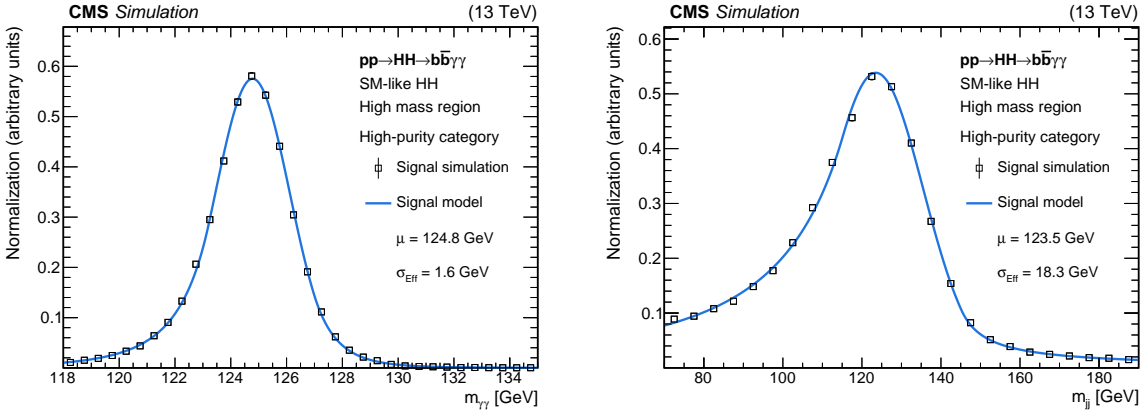
Figure 6: Signal shapes for $m_{\gamma\gamma}$ (left) and m_{jj} (right) in the SM HH nonresonant sample after full analysis selection in the high-mass and HPC region. The solid line shows a fit to the simulated data points with a double-sided Crystal Ball function. The normalization of the shapes is arbitrary.

5.3 Background modeling

The total background model is obtained as a sum of the $n\gamma + \text{jets}$ background continuum PD and single-Higgs boson production PDs, the latter being normalized to their SM production cross sections.

For both the resonant and nonresonant analyses the $n\gamma + \text{jets}$ continuum is described using polynomials in the Bernstein basis [55]. The data control sample described in Section 5.2 is used to define the appropriate order of the polynomial function for the one-dimensionnal PDs of the $n\gamma + \text{jets}$ background continuum. For each search we randomly select from the control

sample a number of events equal to the total number of events observed in data. A second-order Bernstein polynomial fits the data well. In categories with fewer events, occurring in the resonant analysis, a first-order Bernstein polynomial is used. This choice of the background PD is tested for possible biases in the signal extraction by comparing it to other possible background models, such as exponentials and Laurent polynomials. The bias from the chosen PD is always found to be smaller than the statistical uncertainty in the fit, and can be safely neglected [2]. The correlation between $m_{\gamma\gamma}$ and m_{jj} was measured in the data control sample and found to be compatible with zero.

The SM single-Higgs boson background contribution is estimated using a PD fitted to simulated samples. For all production mechanisms, the $m_{\gamma\gamma}$ distribution is modeled by a double-sided CB function. The m_{jj} modeling depends on the production mechanism: for ggH and VBF H production m_{jj} is modeled with a Bernstein polynomial; for VH production a double-sided CB function is expected to describe the line shape of the hadronic decays of vector bosons; for $t\bar{t}H$ and $b\bar{b}H$ a double-sided CB function is also used. Like the signal modeling, the final 2D SM single-Higgs boson model is an independent product of models of the $m_{\gamma\gamma}$ and m_{jj} distributions. This background contribution is explicitly considered only for the nonresonant search, since for the resonant one it is severely reduced by a tight selection window on $\widetilde{M}_X$. The residual events are accounted for by the continuum background models for the $m_{\gamma\gamma}$ and m_{jj} variables. The one-dimensional projections of the background-plus-signal fits in the signal regions of the nonresonant analysis are shown in Figs. 7 and 8.
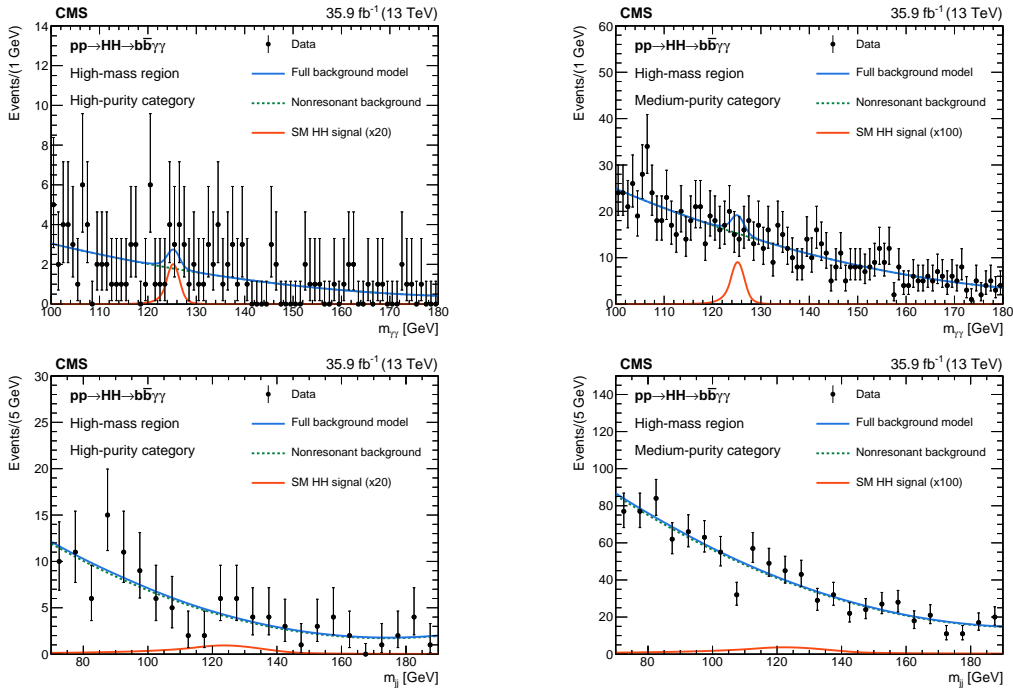

Figure 7: Background fits for the SM HH nonresonant analysis selection in the HM region. The plots on the left (right) show the distributions in the HPC (MPC) region. Top plots show the $m_{\gamma\gamma}$ spectra and bottom ones m_{jj} ones. The green dashed line represents the nonresonant part of the expected background; the solid blue line represents the full background modeling PD, i.e., the sum of nonresonant background and SM single-Higgs boson contributions scaled to their cross sections; and the solid red line represents the SM-like HH production, normalized to its SM cross section times a scaling factor specified in the legend.
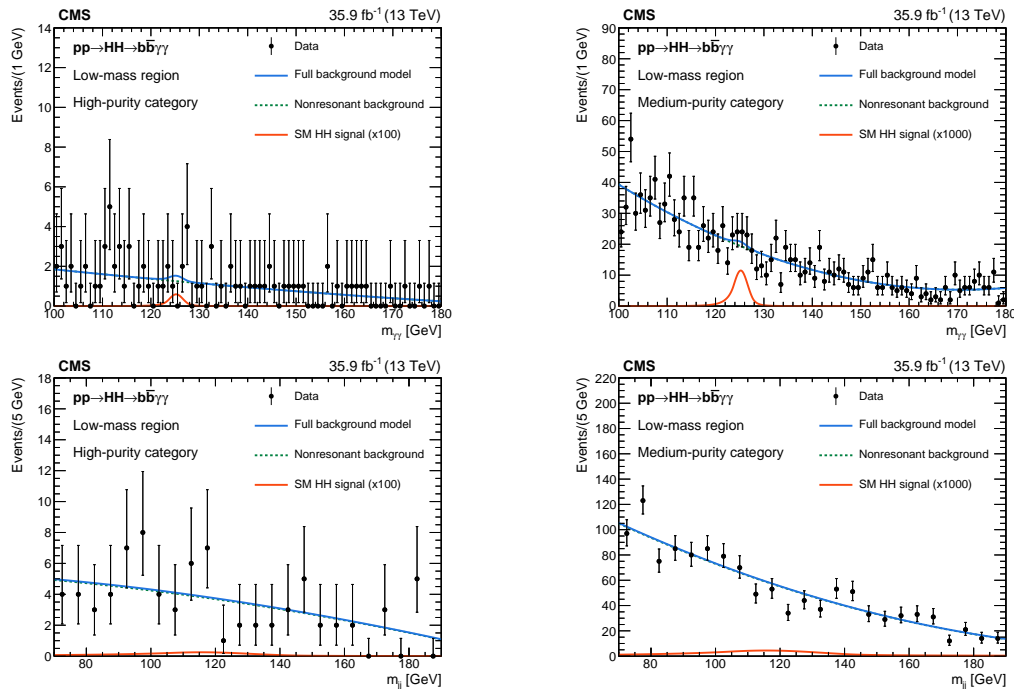
Figure 8: Background fits for the SM HH nonresonant analysis selection in the LM region. The plots on the left (right) show the distributions in the HPC (MPC) region. Top plots show the $m_{\gamma\gamma}$ spectra and bottom ones the m_{jj} ones. The green dashed line represents the nonresonant part of the expected background; the solid blue line represents the full background modeling PD, i.e., the sum of nonresonant background and SM single-Higgs boson contributions scaled to their cross sections; and the solid red line represents the SM-like HH production, normalized to its SM cross section times a scaling factor specified in the legend.

6 Fitting procedure and systematic uncertainties

A likelihood function is defined based on the total PD including the backgrounds, signal hypothesis, and the data. Then an unbinned maximum likelihood fit is performed to the 2D $m_{\gamma\gamma} - m_{jj}$ data distribution. The parameters for the signal yield and for the background-only PD are constrained in the fit. Uniform priors are used to parametrize the nonresonant background PD and log-normal priors are assumed for the single-Higgs boson background parametrizing our degree of uncertainty in the exact SM production cross section. When converting the fitted yields into production cross sections, we use simulation to estimate the selection efficiency for the signal. The difference between the simulation and the data is taken into account through parameters included in the likelihood function. Parameters related to the systematic uncertainties (nuisance parameters) are varied in the fit according to a log-normal PD function and can be classified according to their impact on the analysis. The uncertainty in the estimation of the integrated luminosity modifies the total expected signal normalization and is taken to be 2.5% [70]. Other systematic uncertainties modify the efficiency of the signal selection or impact the signal or the Higgs boson PD.

The photon-related uncertainties are discussed in Ref. [55]. The photon energy scale (PES) is known at a sub-percent level and the photon energy resolution (PER) is known with 5% precision. A 2% normalization uncertainty is estimated in the offline diphoton selection efficiency and in the trigger efficiency, while 1% is assigned to quantify the uncertainty on the photon identification efficiency.

The uncertainties in the jet energy scale (JES) and jet energy resolution (JER) are accounted for by changing the jet response by one standard deviation for each source [61]. They impact the average m_{jj} peak position by approximately 1% and the peak resolution by 5%. The effects on the signal acceptance are also accounted for.

To use the b tagging score as an input to the classification MVA, its simulated distribution is matched to data by applying differential scale factors that depend on the jet p_T and η [60]. The uncertainty in the efficiency of the categorization MVA is estimated by varying the b tagging differential scale factors within one standard deviation of their uncertainties [60]. The impacts of PES, PER, JES, and JER on the MVA classification procedure have been found to be negligible. Those four sources have, nevertheless, a mild impact on the $\widetilde{M}_X$–based categorization.

Theoretical uncertainties have been applied to the normalization of the single-Higgs boson background, but not on BSM signals. When we consider the SM-like search and parametrize the BSM cross section $\sigma_{gg\to HH}^{BSM}$ by the ratio $\mu_{HH} = \sigma_{gg\to HH}^{BSM}/\sigma_{gg\to HH}^{SM}$, the theoretical uncertainties on $\sigma_{gg\to HH}^{SM}$ are included in the likelihood. The following sources are considered correlated for all the single-Higgs boson channels (except b$\bar{\text{b}}$H) and the double-Higgs boson channel in line with the recommendations from Ref. [6]: the scale dependence of higher-order terms; the impact from the choice of PDF quadratically summed with the uncertainty on α_S; and, in the case of the HH channel, the uncertainties related to the inclusion of m_t into the cross section calculations. Finally, for the b$\bar{\text{b}}$H channel all sources are summed together including also the uncertainty on the b quark mass.

The systematic uncertainties are summarized in Table 4. The correlations between different categories are taken into account. The analysis is limited by the statistical precision. For example, the systematic uncertainties worsen the expected cross section limits by 3% for the search performed assuming a SM-like signal.

7 Results

No evidence for HH production is observed in the data. Upper limits on the production cross section of a pair of Higgs bosons times the branching fraction $\mathcal{B}(\text{HH} \to \gamma\gamma\text{b}\bar{\text{b}})$ are computed using the modified frequentist approach for confidence levels (CL$_s$), taking the profile likelihood as a test statistic [71–74] in the asymptotic approximation. The limits are subsequently compared to theoretical predictions assuming SM branching fractions for Higgs boson decays.

7.1 Resonant signal

The observed and median expected upper limits at 95% confidence level (CL) are shown in Fig. 9, for the pp $\to$ X $\to$ HH $\to \gamma\gamma\text{b}\bar{\text{b}}$ process assuming spin-0 and a spin-2 resonances. The data exclude a cross section of 0.23 to 4.2 fb depending on m_X and the spin hypothesis.

The results are compared with the cross sections for bulk radion and bulk KK graviton production in WED models. In analogy with the Higgs boson, the hypothesized bulk radion field is expected to be predominantly produced through gluon-gluon fusion [75] and the cross section is calculated at NLO accuracy in QCD, using the recipe suggested in Ref. [76]. The theoretical input used in this letter is identical to the one from a previous CMS analysis [23]. More details can be found in Ref. [77]. The production cross section in this model is proportional to $1/\Lambda_R^2$, where Λ_R is the scale parameter of the theory. The analysis at $\sqrt{s} = 8$ TeV [23] already excluded a radion resonance up to 980 GeV for the scale parameter $\Lambda_R = 1$ TeV, but had no sensitivity for $\Lambda_R = 3$ TeV. In this analysis the observed limits are able to exclude radion reso-

Table 4: Summary of systematic uncertainties.

Sources of systematic uncertainties	Type	Value (%)
Integrated luminosity	Normalization	2.5
Photon related uncertainties		
Diphoton selection (with trigger uncertainties and PES)	Normalization	2.0
Photon identification	Normalization	1.0
PES ($\frac{\Delta m_{\gamma\gamma}}{m_{\gamma\gamma}}$)	Shape	0.5
PER ($\frac{\Delta\sigma_{\gamma\gamma}}{\sigma_{\gamma\gamma}}$)	Shape	5.0
Jet related uncertainties		
Dijet selection (JES+JER)	Normalization	0.5
JES ($\frac{\Delta m_{jj}}{m_{jj}}$)	Shape	1.0
JER ($\frac{\Delta\sigma_{jj}}{\sigma_{jj}}$)	Shape	5.0
Resonant analysis specific uncertainties		
Mass window selection (JES+JER)	Normalization	3.0
Classification MVA – b tagging (HPC)	Normalization	10–19
Classification MVA – b tagging (MPC)	Normalization	3–9
Nonresonant analysis specific uncertainties		
$\widetilde{M}_X$ Classification	Normalization	0.5
Classification MVA – b tagging (HPC)	Normalization	10–19
Classification MVA – b tagging (MPC)	Normalization	3–9
Theoretical uncertainties in the SM single-Higgs boson production		
QCD missing orders (ggH, VBF H , VH, t$\bar{\text{t}}$H)	Normalization	0.4–5.8
PDF and α_S uncertainties (ggH, VBF H , VH, t$\bar{\text{t}}$H)	Normalization	1.6–3.6
Theoretical uncertainty b$\bar{\text{b}}$H	Normalization	20
Theoretical uncertainties in the SM HH boson production		
QCD missing orders	Normalization	4.3–6
PDF and α_S uncertainties	Normalization	3.1
m_t effects	Normalization	5

nances, assuming $\Lambda_R = 2\,\text{TeV}$, for all points below $m_X = 840\,\text{GeV}$ and, assuming $\Lambda_R = 3\,\text{TeV}$, below $m_X = 540\,\text{GeV}$. The couplings of the gravitons to matter fields are defined by $\kappa/\overline{M_{Pl}}$, with $\overline{M_{Pl}} \equiv M_{Pl}/\sqrt{8\pi}$ being the reduced Planck mass and κ the warp factor of the metric. Assuming $\kappa/\overline{M_{Pl}} = 1.0$, gravitons are excluded within the range $290 < m_X < 810\,\text{GeV}$, while assuming $\kappa/\overline{M_{Pl}} = 0.5$, the exclusion range is $350 < m_X < 530\,\text{GeV}$.

The events in a signal region defined by $122 < m_{\gamma\gamma} < 128\,\text{GeV}$ and $90 < m_{jj} < 160\,\text{GeV}$ are shown as a function of m_X in Fig. 10 and compared to three different resonant signal hypotheses with theory parameters chosen in such a way that their cross sections are close to the excluded ones. The vertical lines show the mass windows that are used to select in m_X and set the limits shown in Fig. 9.

7.2 Nonresonant signal

The observed (expected) 95% CL upper limit on the SM-like $pp \rightarrow HH \rightarrow \gamma\gamma b\bar{b}$ process is 2.0 (1.6 fb), and 0.79 (0.63 pb) for the total ggHH production cross section assuming SM Higgs boson branching fractions. The results can also be interpreted in terms of observed (expected) upper limits on μ_{HH} of 24 (19). The constraint on μ_{HH} is a factor of three more restrictive that
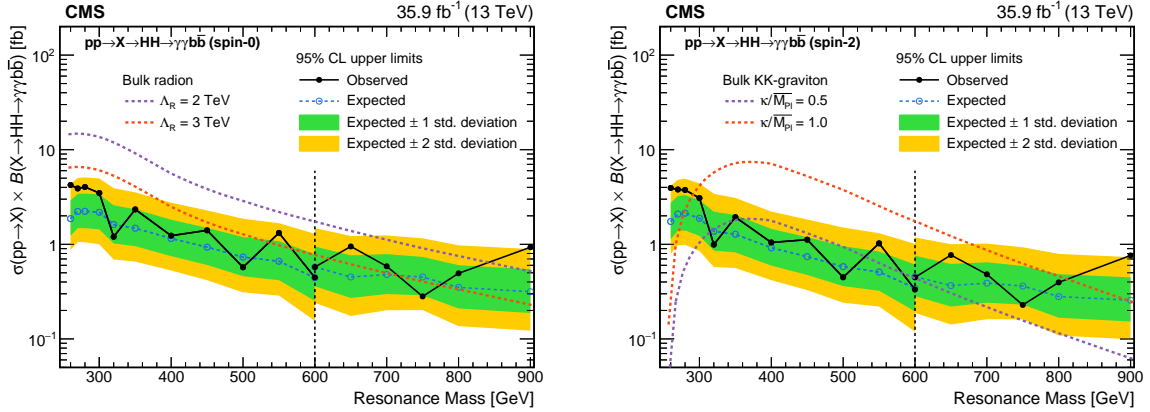
Figure 9: Observed and expected 95% CL upper limits on the product of cross section and branching fraction $\sigma(\text{pp} \to \text{X})\mathcal{B}(\text{X} \to \text{HH} \to \gamma\gamma\text{b}\bar{\text{b}})$ obtained through a combination of the two analysis categories (HPC and MPC) for spin-0 (left) and spin-2 (right) hypotheses. The green and yellow bands represent, respectively, the one and two standard deviation extensions beyond the expected limit. Also shown are theoretical predictions corresponding to WED models for bulk radions (top) and bulk KK gravitons (bottom). The vertical dashed lines show the boundary between the low- and high-mass regions. The limits for $m_\text{X} = 600\,\text{GeV}$ are shown for both methods.

the previous search [23].

An additional study is performed including both VBF HH and ggHH production mechanisms in the definition of the scaling factor

$$\mu_\text{HH}^\text{ext} = \frac{\sigma_{\text{gg}\to\text{HH}}^\text{BSM} + \sigma_{\text{VBF HH}}^\text{BSM}}{\sigma_{\text{gg}\to\text{HH}}^\text{SM} + \sigma_{\text{VBF HH}}^\text{SM}} \tag{3}$$

where $\sigma_{\text{VBF HH}}^\text{SM} = 1.64^{+0.05}_{-0.06}$ fb [6]. The expected sensitivity of the analysis for μ_HH^ext improves by 1.3% compared to μ_HH. The improvement is smaller than the relative contribution of the VBF production cross section to the total one in the SM because of the nonoptimal selection efficiency of this analysis for the VBF events, as explained in Section 5.

The results are also interpreted in the context of Higgs boson anomalous couplings. Limits on the different BSM benchmark hypotheses (listed in Table 1) are shown in Fig. 11 (top). Using the limits on the benchmark hypotheses and the map between the clusters and the points in the 5D BSM parameter space, one can estimate the constraints provided by these data in different regions of phase space. It is important to stress that the same analysis categories are used for the SM-like search and for all BSM nonresonant searches. The differences between the limits come only from the kinematic properties of the benchmark signal hypotheses. For instance, the tightest constraint is placed on the benchmark 2 hypothesis, which features a m_HH spectrum that extends above 1 TeV owing to large contributions from dimension-6 operators. The least restrictive constraint is on benchmark 7 that describes models with large values of κ_λ, where the m_HH spectrum peaks below 300 GeV. For benchmark 2 most of the events would be observed in the HM categories, while for benchmark 7 most events fall in the LM categories. Assuming equal cross sections, benchmark hypothesis 2 has a much better signal-over-background ratio than benchmark hypothesis 7. In the intermediate case of SM-like production it was observed that the HM categories have the best sensitivity.

We reweight the benchmark samples to model different values of the SM coupling modifier κ_λ, with κ_t and other BSM parameters fixed to their SM values. In Fig. 11 (bottom), 95% CL limits
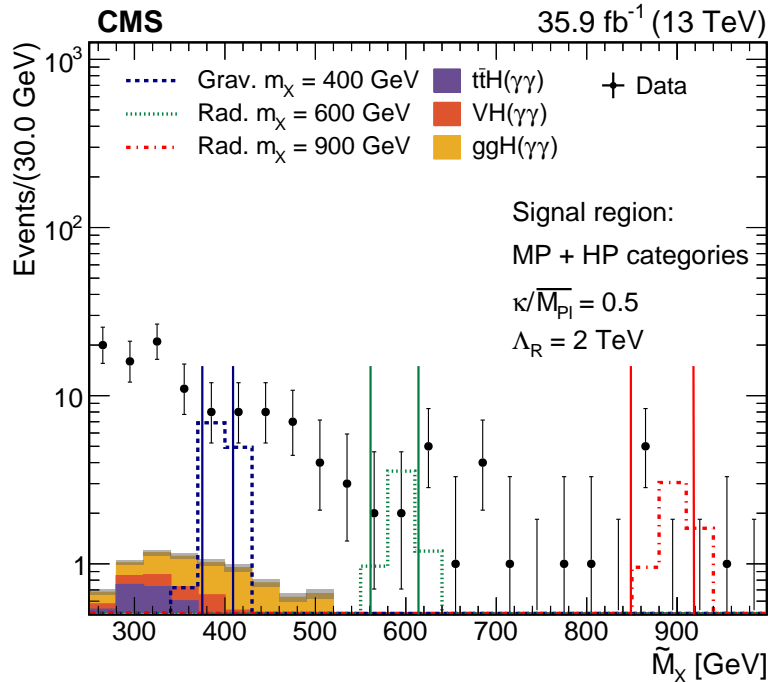
Figure 10: Data (dots) with statistical uncertainties (vertical black lines around the dots) histogrammed in bins of $\widetilde{M}_X$ are overlaid onto expected Monte Carlo simulated distributions for three single-Higgs bosons samples (t$\bar{\text{t}}$H, VH, and ggH) and three different resonant signal hypotheses. The data-driven backgrounds, dominated by $n\gamma + \text{jets}$, are not shown and are specific to the analysis categories. The events are selected in the signal region defined by $122 < m_{\gamma\gamma} < 128\,\text{GeV}$ and $90 < m_{\text{jj}} < 160\,\text{GeV}$ and use the photons and jets selections summarized in Table 2. The MP and HP categories are merged together. The signals are normalized to the theory cross section calculated with the parameters shown in the figure and assuming a narrow width approximation. The vertical lines shows the mass windows that are used to select in m_X and set the limits shown in Fig. 9

on the nonresonant Higgs boson pair production cross sections are shown as a function of κ_λ. Assuming that the top quark Yukawa coupling is SM-like ($\kappa_t = 1$), the analysis constrains κ_λ to values between -11 and 17.

8 Summary

A search is performed by the CMS Collaboration for the resonant and nonresonant production of a pair of Higgs bosons in the decay channel HH $\rightarrow \gamma\gamma$b$\bar{\text{b}}$, based on an integrated luminosity of $35.9\,\text{fb}^{-1}$ of pp collisions collected at $\sqrt{s} = 13\,\text{TeV}$ in 2016. No statistically significant deviations from the standard model (SM) predictions are found. Upper limits at a 95% CL are set on the cross sections for the production of new particles decaying to two Higgs bosons in the mass range between 250 and 900 GeV, under the spin-0 and spin-2 hypotheses. In the case of beyond SM predictions, based on the assumption of the existence of a warped extra dimension, we exclude the radion (spin-0) signal hypothesis, assuming the scale parameter $\Lambda_R = 3\,\text{TeV}$, for all masses below $m_X = 540\,\text{GeV}$, and the KK graviton (spin-2) hypothesis for the mass range $290 < m_X < 810\,\text{GeV}$, assuming $\kappa/\overline{M}_{\text{Pl}} = 1.0$ ($\overline{M}_{\text{Pl}}$ being the reduced Planck mass and κ the warp factor of the metric). For nonresonant production with SM-like kinematics, a 95% CL upper limit of 2.0 fb is set on $\sigma(\text{pp} \rightarrow \text{HH} \rightarrow \gamma\gamma\text{b}\bar{\text{b}})$, corresponding to about 24 times the SM
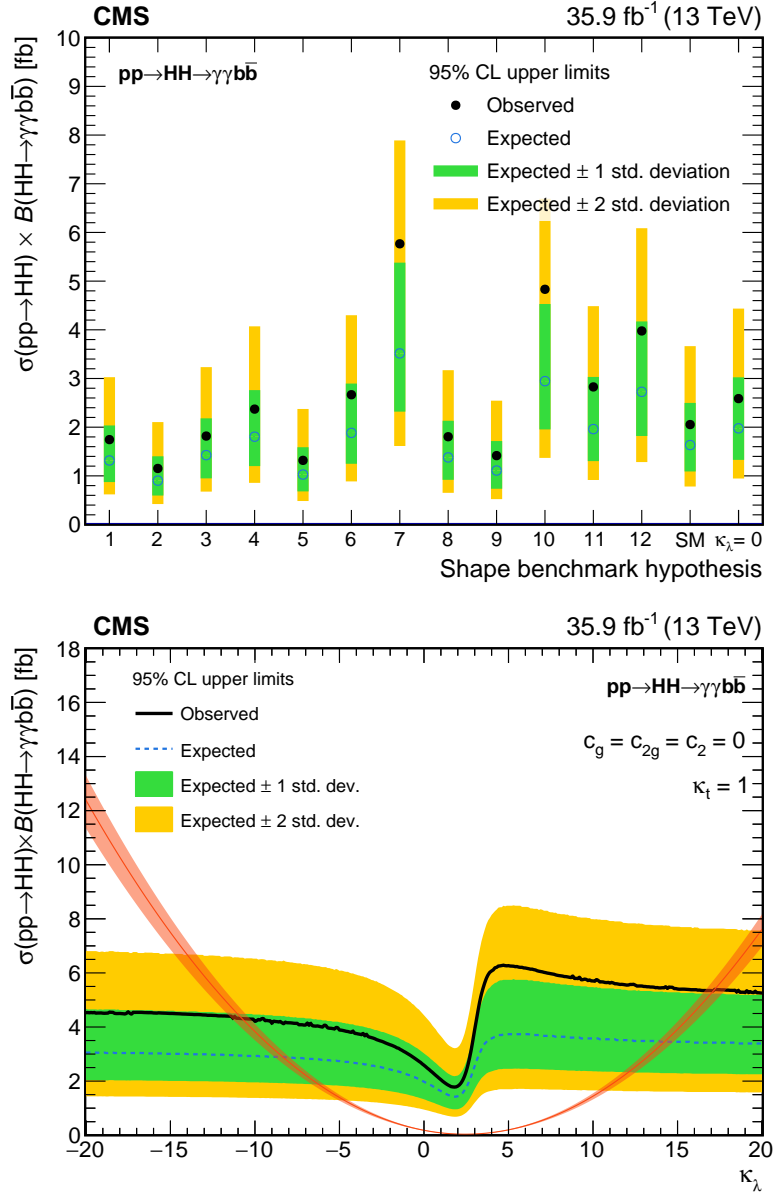
Figure 11: Expected and observed 95% CL upper limits on the SM-like HH production cross section times $\mathcal{B}(HH \rightarrow \gamma\gamma b\bar{b})$ obtained for different nonresonant benchmark models (defined in Table 1) (top); for different values of the κ_λ (bottom). The green and yellow bands represent, respectively, the one and two standard deviation extensions beyond the expected limit. The red line in the bottom plot shows the prediction of theory with the associated uncertainties shown as the orange band.

prediction. Anomalous couplings of the Higgs boson are also investigated, as well as the vector boson fusion HH production process. Values of the effective Higgs boson self-coupling κ_λ are constrained to be within the range $-11 < \kappa_\lambda < 17$ at 95% CL, assuming all other Higgs boson couplings to be at their SM values. The direct constraints reported on κ_λ are the most restrictive to date.

Acknowledgments

References

[1] ATLAS Collaboration, "Observation of a new particle in the search for the standard model Higgs boson with the ATLAS detector at the LHC", *Phys. Lett. B* **716** (2012) 1, `doi:10.1016/j.physletb.2012.08.020,arXiv:1207.7214`.

[2] CMS Collaboration, "Observation of a new boson at a mass of 125 GeV with the CMS experiment at the LHC", *Phys. Lett. B* **716** (2012) 30, `doi:10.1016/j.physletb.2012.08.021,arXiv:1207.7235`.

[3] CMS Collaboration, "Observation of a new boson with mass near 125 GeV in pp collisions at $\sqrt{s}$ = 7 and 8 TeV", *JHEP* **06** (2013) 081, `doi:10.1007/JHEP06(2013)081`, `arXiv:1303.4571`.

[4] F. Englert and R. Brout, "Broken symmetries and the masses of gauge bosons", *Phys. Rev. Lett.* **13** (1964) 321, `doi:10.1103/PhysRevLett.13.321`.

[5] P. W. Higgs, "Broken symmetries and the masses of gauge bosons", *Phys. Rev. Lett.* **13** (1964) 508, `doi:10.1103/PhysRevLett.13.508`.

[6] D. de Florian et al., "Handbook of LHC Higgs cross sections: 4. Deciphering the nature of the Higgs sector", CERN Report CERN-2017-002-M, 2016. `doi:10.23731/CYRM-2017-002`, `arXiv:1610.07922`.

[7] D. de Florian and J. Mazzitelli, "Higgs boson pair production at next-to-next-to-leading order in QCD", *Phys. Rev. Lett.* **111** (2013) 201801, `doi:10.1103/PhysRevLett.111.201801`, `arXiv:1309.6594`.

[8] J. Baglio et al., "The measurement of the Higgs self-coupling at the LHC: theoretical status", *JHEP* **04** (2013) 151, `doi:10.1007/JHEP04(2013)151`, `arXiv:1212.5581`.

[9] L. Randall and R. Sundrum, "Large mass hierarchy from a small extra dimension", *Phys. Rev. Lett.* **83** (1999) 3370, `doi:10.1103/PhysRevLett.83.3370`, `arXiv:hep-ph/9905221`.

[10] W. D. Goldberger and M. B. Wise, "Modulus stabilization with bulk fields", *Phys. Rev. Lett.* **83** (1999) 4922, `doi:10.1103/PhysRevLett.83.4922`, `arXiv:hep-ph/9907447`.

[11] H. Davoudiasl, J. L. Hewett, and T. G. Rizzo, "Phenomenology of the Randall–Sundrum gauge hierarchy model", *Phys. Rev. Lett.* **84** (2000) 2080, `doi:10.1103/PhysRevLett.84.2080`, `arXiv:hep-ph/9909255`.

[12] A. L. Fitzpatrick, J. Kaplan, L. Randall, and L.-T. Wang, "Searching for the Kaluza–Klein graviton in bulk RS models", *JHEP* **09** (2007) 013, `doi:10.1088/1126-6708/2007/09/013`, `arXiv:hep-ph/0701150`.

[13] D. O'Connell, M. J. Ramsey-Musolf, and M. B. Wise, "Minimal extension of the standard model scalar sector", *Phys. Rev. D* **75** (2007) 037701, `doi:10.1103/PhysRevD.75.037701`, `arXiv:hep-ph/0611014`.

[14] G. C. Branco et al., "Theory and phenomenology of two-Higgs-doublet models", *Phys. Rept.* **516** (2012) 1, `doi:10.1016/j.physrep.2012.02.002`, `arXiv:1106.0034`.

[15] A. Djouadi, "The anatomy of electroweak symmetry breaking. Tome II: the Higgs bosons in the Minimal Supersymmetric model", *Phys. Rept.* **459** (2008) 1, `doi:10.1016/j.physrep.2007.10.005`, `arXiv:hep-ph/0503173`.

[16] H. Georgi and M. Machacek, "Doubly charged Higgs bosons", *Nucl. Phys. B* **262** (1985) 463, `doi:10.1016/0550-3213(85)90325-6`.

[17] S. Dawson, A. Ismail, and I. Low, "What's in the loop? The anatomy of double Higgs production", *Phys. Rev. D* **91** (2015) 115008, `doi:10.1103/PhysRevD.91.115008`, `arXiv:1504.05596`.

[18] R. Gröber and M. Mühlleitner, "Composite Higgs boson pair production at the LHC", *JHEP* **06** (2011) 020, `doi:10.1007/JHEP06(2011)020`, `arXiv:1012.1562`.

[19] ATLAS Collaboration, "Search for Higgs boson pair production in the $\gamma\gamma b\bar{b}$ final state using pp collision data at $\sqrt{s} = 8\,\text{TeV}$ from the ATLAS detector", *Phys. Rev. Lett.* **114** (2015) 081802, `doi:10.1103/PhysRevLett.114.081802`, `arXiv:1406.5053`.

[20] ATLAS Collaboration, "Search for Higgs boson pair production in the $b\bar{b}b\bar{b}$ final state from pp collisions at $\sqrt{s} = 8\,\text{TeV}$ with the ATLAS detector", *Eur. Phys. J. C* **75** (2015) 412, `doi:10.1140/epjc/s10052-015-3628-x`, `arXiv:1506.00285`.

[21] ATLAS Collaboration, "Searches for Higgs boson pair production in the $HH \to b\bar{b}\tau\tau$, $\gamma\gamma WW^*$, $\gamma\gamma b\bar{b}$, $b\bar{b}b\bar{b}$ channels with the ATLAS detector", *Phys. Rev. D* **92** (2015) 092004, `doi:10.1103/PhysRevD.92.092004`, `arXiv:1509.04670`.

[22] ATLAS Collaboration, "Search for pair production of Higgs bosons in the $b\bar{b}b\bar{b}$ final state using proton–proton collisions at $\sqrt{s} = 13\,\text{TeV}$ with the ATLAS detector", *Phys. Rev. D* **94** (2016) 052002, `doi:10.1103/PhysRevD.94.052002`, `arXiv:1606.04782`.

[23] CMS Collaboration, "Search for two Higgs bosons in final states containing two photons and two bottom quarks in proton-proton collisions at 8 TeV", *Phys. Rev. D* **94** (2016) 052012, `doi:10.1103/PhysRevD.94.052012`, `arXiv:1603.06896`.

[24] CMS Collaboration, "Search for resonant pair production of Higgs bosons decaying to two bottom quark-antiquark pairs in proton-proton collisions at 8 TeV", *Phys. Lett. B* **749** (2015) 560, `doi:10.1016/j.physletb.2015.08.047`, `arXiv:1503.04114`.

[25] CMS Collaboration, "Search for a massive resonance decaying to a pair of Higgs bosons in the four b quark final state in proton-proton collisions at $\sqrt{s} = 13\,\text{TeV}$", *Phys. Lett. B* **781** (2018) 244, `doi:10.1016/j.physletb.2018.03.084`, `arXiv:1710.04960`.

[26] CMS Collaboration, "Search for Higgs boson pair production in the $b\bar{b}\tau\tau$ final state in proton-proton collisions at $\sqrt{s} = 8\,\text{TeV}$", *Phys. Rev. D* **96** (2017) 072004, `doi:10.1103/PhysRevD.96.072004`, `arXiv:1707.00350`.

[27] CMS Collaboration, "Search for Higgs boson pair production in events with two bottom quarks and two tau leptons in proton-proton collisions at $\sqrt{s} = 13\,\text{TeV}$", *Phys. Lett. B* **778** (2018) 101, `doi:10.1016/j.physletb.2018.01.001`, `arXiv:1707.02909`.

[28] CMS Collaboration, "Search for resonant and nonresonant Higgs boson pair production in the $b\bar{b}\ell\nu\ell\nu$ final state in proton-proton collisions at $\sqrt{s} = 13\,\text{TeV}$", *JHEP* **01** (2018) 054, `doi:10.1007/JHEP01(2018)054`, `arXiv:1708.04188`.

[29] CMS Collaboration, "The CMS experiment at the CERN LHC", *JINST* **3** (2008) S08004, `doi:10.1088/1748-0221/3/08/S08004`.

[30] CMS Collaboration, "The CMS trigger system", *JINST* **12** (2017) P01020, `doi:10.1088/1748-0221/12/01/P01020`, `arXiv:1609.02366`.

[31] J. Alwall et al., "The automated computation of tree-level and next-to-leading order differential cross sections, and their matching to parton shower simulations", *JHEP* **07** (2014) 079, `doi:10.1007/JHEP07(2014)079`, `arXiv:1405.0301`.

[32] B. Hespel, D. Lopez-Val, and E. Vryonidou, "Higgs pair production via gluon fusion in the two-Higgs-doublet model", *JHEP* **09** (2014) 124, `doi:10.1007/JHEP09(2014)124`, `arXiv:1407.0281`.

[33] R. Frederix et al., "Higgs pair production at the LHC with NLO and parton-shower effects", *Phys. Lett. B* **732** (2014) 142, `doi:10.1016/j.physletb.2014.03.026`, `arXiv:1401.7340`.

[34] A. Buckley et al., "LHAPDF6: parton density access in the LHC precision era", *Eur. Phys. J. C* **75** (2015) 132, `doi:10.1140/epjc/s10052-015-3318-8`, `arXiv:1412.7420`.

[35] S. Carrazza, J. I. Latorre, J. Rojo, and G. Watt, "A compression algorithm for the combination of PDF sets", *Eur. Phys. J. C* **75** (2015) 474, `doi:10.1140/epjc/s10052-015-3703-3`, `arXiv:1504.06469`.

[36] J. Butterworth et al., "PDF4LHC recommendations for LHC Run II", *J. Phys. G* **43** (2016) 023001, `doi:10.1088/0954-3899/43/2/023001`, `arXiv:1510.03865`.

[37] S. Dulat et al., "New parton distribution functions from a global analysis of quantum chromodynamics", *Phys. Rev. D* **93** (2016) 033006, `doi:10.1103/PhysRevD.93.033006`, `arXiv:1506.07443`.

[38] L. A. Harland-Lang, A. D. Martin, P. Motylinski, and R. S. Thorne, "Parton distributions in the LHC era: MMHT 2014 PDFs", *Eur. Phys. J. C* **75** (2015) 204, `doi:10.1140/epjc/s10052-015-3397-6`, `arXiv:1412.3989`.

[39] NNPDF Collaboration, "Parton distributions for the LHC Run II", *JHEP* **04** (2015) 040, `doi:10.1007/JHEP04(2015)040`, `arXiv:1410.8849`.

[40] ATLAS and CMS Collaboration, "Combined measurement of the Higgs boson mass in pp collisions at $\sqrt{s} = 7$ and 8 TeV with the ATLAS and CMS experiments", *Phys. Rev. Lett.* **114** (2015) 191803, `doi:10.1103/PhysRevLett.114.191803`, `arXiv:1503.07589`.

[41] A. Carvalho et al., "Analytical parametrization and shape classification of anomalous HH production in the EFT approach", (2016). `arXiv:1608.06578`.

[42] G. F. Giudice, C. Grojean, A. Pomarol, and R. Rattazzi, "The strongly-interacting light Higgs", *JHEP* **06** (2007) 045, `doi:10.1088/1126-6708/2007/06/045`, `arXiv:hep-ph/0703164`.

[43] J. Grigo, K. Melnikov, and M. Steinhauser, "Virtual corrections to Higgs boson pair production in the large top quark mass limit", *Nucl. Phys. B* **888** (2014) 17, `doi:10.1016/j.nuclphysb.2014.09.003`, `arXiv:1408.2422`.

[44] S. Borowka et al., "Full top quark mass dependence in higgs boson pair production at NLO", *JHEP* **10** (2016) 107, `doi:10.1007/JHEP10(2016)107`, `arXiv:1608.04798`.

[45] A. Carvalho et al., "Higgs pair production: choosing benchmarks with cluster analysis", *JHEP* **04** (2016) 126, `doi:10.1007/JHEP04(2016)126`, `arXiv:1507.02245`.

[46] A. Carvalho et al., "On the reinterpretation of non-resonant searches for Higgs boson pairs", (2017). `arXiv:1710.08261`.

[47] D. Fäh and N. Greiner, "Diphoton production in association with two bottom jets", *Eur. Phys. J. C* **77** (2017) 750, `doi:10.1140/epjc/s10052-017-5296-5`, `arXiv:1706.08309`.

[48] P. Nason, "A new method for combining NLO QCD with shower Monte Carlo algorithms", *JHEP* **11** (2004) 040, `doi:10.1088/1126-6708/2004/11/040`, `arXiv:hep-ph/0409146`.

[49] S. Frixione, P. Nason, and C. Oleari, "Matching NLO QCD computations with parton shower simulations: the POWHEG method", *JHEP* **11** (2007) 070, `doi:10.1088/1126-6708/2007/11/070`, `arXiv:0709.2092`.

[50] S. Alioli, P. Nason, C. Oleari, and E. Re, "A general framework for implementing NLO calculations in shower Monte Carlo programs: the POWHEG BOX", *JHEP* **06** (2010) 043, `doi:10.1007/JHEP06(2010)043`, `arXiv:1002.2581`.

[51] E. Bagnaschi, G. Degrassi, P. Slavich, and A. Vicini, "Higgs production via gluon fusion in the POWHEG approach in the SM and in the MSSM", *JHEP* **02** (2012) 088, `doi:10.1007/JHEP02(2012)088`, `arXiv:1111.2854`.

[52] T. Sjöstrand et al., "An introduction to PYTHIA 8.2", *Comput. Phys. Commun.* **191** (2015) 159, `doi:10.1016/j.cpc.2015.01.024`, `arXiv:1410.3012`.

[53] CMS Collaboration, "Event generator tunes obtained from underlying event and multiparton scattering measurements", *Eur. Phys. J. C* **76** (2016) 155, `doi:10.1140/epjc/s10052-016-3988-x`, `arXiv:1512.00815`.

[54] GEANT4 Collaboration, "GEANT4—a simulation toolkit", *Nucl. Instrum. Meth. A* **506** (2003) 250, `doi:10.1016/S0168-9002(03)01368-8`.

[55] CMS Collaboration, "Observation of the diphoton decay of the Higgs boson and measurement of its properties", *Eur. Phys. J. C* **74** (2014) 3076, `doi:10.1140/epjc/s10052-014-3076-z`, `arXiv:1407.0558`.

[56] CMS Collaboration, "Performance of photon reconstruction and identification with the CMS detector in proton-proton collisions at $\sqrt{s} = 8$ TeV", *JINST* **10** (2015) P08010, `doi:10.1088/1748-0221/10/08/P08010`, `arXiv:1502.02702`.

[57] CMS Collaboration, "Particle-flow reconstruction and global event description with the CMS detector", *JINST* **12** (2017) P10003, `doi:10.1088/1748-0221/12/10/P10003`, `arXiv:1706.04965`.

[58] M. Cacciari, G. P. Salam, and G. Soyez, "The anti-k_T jet clustering algorithm", *JHEP* **04** (2008) 063, `doi:10.1088/1126-6708/2008/04/063`, `arXiv:0802.1189`.

[59] M. Cacciari, G. P. Salam, and G. Soyez, "FastJet user manual", *Eur. Phys. J. C* **72** (2012) 1896, `doi:10.1140/epjc/s10052-012-1896-2`, `arXiv:1111.6097`.

[60] CMS Collaboration, "Identification of heavy-flavour jets with the CMS detector in pp collisions at 13 TeV", *JINST* **13** (2017) P05011, `doi:10.1088/1748-0221/13/05/P05011`, `arXiv:1712.07158`.

[61] CMS Collaboration, "Determination of jet energy calibration and transverse momentum resolution in CMS", *JINST* **6** (2011) P11002, `doi:10.1088/1748-0221/6/11/P11002`, `arXiv:1107.4277`.

[62] CMS Collaboration, "Evidence for the Higgs boson decay to a bottom quark-antiquark pair", *Phys. Lett. B* **780** (2018) 501, `doi:10.1016/j.physletb.2018.02.050`, `arXiv:1709.07497`.

[63] N. Kumar and S. P. Martin, "LHC search for di-Higgs decays of stoponium and other scalars in events with two photons and two bottom jets", *Phys. Rev. D* **90** (2014) 055007, `doi:10.1103/PhysRevD.90.055007`, `arXiv:1404.0996`.

[64] S. Bolognesi et al., "Spin and parity of a single-produced resonance at the LHC", *Phys. Rev. D* **86** (2012) 095031, `doi:10.1103/PhysRevD.86.095031`, `arXiv:1208.4018`.

[65] M. V. Chizhov, V. A. Bednyakov, and J. A. Budagov, "On resonance search in dijet events at the LHC", (2011). `arXiv:1106.4161`.

[66] A. Azatov, R. Contino, G. Panico, and M. Son, "Effective field theory analysis of double Higgs boson production via gluon fusion", *Phys. Rev. D* **92** (2015) 035001, `doi:10.1103/PhysRevD.92.035001`, `arXiv:1502.00539`.

[67] M. Gouzevitch et al., "Scale-invariant resonance tagging in multijet events and new physics in Higgs pair production", *JHEP* **07** (2013) 148, `doi:10.1007/JHEP07(2013)148`, `arXiv:1303.6636`.

[68] H. Voss, A. Höcker, J. Stelzer, and F. Tegenfeldt, "TMVA, the toolkit for multivariate data analysis with ROOT", in *XIth International Workshop on Advanced Computing and Analysis Techniques in Physics Research (ACAT)*, p. 40. 2007. `arXiv:physics/0703039`.

[69] M. J. Oreglia, "A study of the reactions $\psi' \to \gamma\gamma\psi$". PhD thesis, Stanford University, 1980. SLAC Report SLAC-R-236.

[70] CMS Collaboration, "CMS luminosity measurements for the 2016 data taking period", CMS Physics Analysis Summary CMS-PAS-LUM-17-001, CERN, 2017.

[71] A. L. Read, "Presentation of search results: the CL$_s$ technique", *J. Phys. G* **28** (2002) 2693, `doi:10.1088/0954-3899/28/10/313`.

[72] T. Junk, "Confidence level computation for combining searches with small statistics", *Nucl. Instrum. Meth. A* **434** (1999) 435, `doi:10.1016/S0168-9002(99)00498-2`, `arXiv:hep-ex/9902006`.

[73] G. Cowan, K. Cranmer, E. Gross, and O. Vitells, "Asymptotic formulae for likelihood-based tests of new physics", *Eur. Phys. J. C* **71** (2011) 1554, `doi:10.1140/epjc/s10052-011-1554-0`, `arXiv:1007.1727`. [Erratum: `doi:10.1140/epjc/s10052-013-2501-z`].

[74] ATLAS and CMS Collaborations, "Procedure for the LHC Higgs boson search combination in summer 2011", Technical Report CMS-NOTE-2011-005, ATL-PHYS-PUB-2011-11, 2011.

[75] U. Mahanta and A. Datta, "Search prospects of light stabilized radions at Tevatron and LHC", *Phys. Lett. B* **483** (2000) 196, `doi:10.1016/S0370-2693(00)00560-8`, `arXiv:hep-ph/0002183`.

[76] G. F. Giudice, R. Rattazzi, and J. D. Wells, "Graviscalars from higher-dimensional metrics and curvature-Higgs mixing", *Nucl. Phys. B* **595** (2001) 250, `doi:10.1016/S0550-3213(00)00686-6`, `arXiv:hep-ph/0002178`.

[77] A. Carvalho, "Gravity particles from warped extra dimensions, predictions for LHC", (2014). `arXiv:1404.0102`.

A   The CMS Collaboration

Yerevan Physics Institute, Yerevan, Armenia
A.M. Sirunyan, A. Tumasyan

Institut für Hochenergiephysik, Wien, Austria
W. Adam, F. Ambrogi, E. Asilar, T. Bergauer, J. Brandstetter, E. Brondolin, M. Dragicevic, J. Erö, A. Escalante Del Valle, M. Flechl, M. Friedl, R. Frühwirth[1], V.M. Ghete, J. Grossmann, J. Hrubec, M. Jeitler[1], A. König, N. Krammer, I. Krätschmer, D. Liko, T. Madlener, I. Mikulec, E. Pree, N. Rad, H. Rohringer, J. Schieck[1], R. Schöfbeck, M. Spanring, D. Spitzbart, A. Taurok, W. Waltenberger, J. Wittmann, C.-E. Wulz[1], M. Zarucki

Institute for Nuclear Problems, Minsk, Belarus
V. Chekhovsky, V. Mossolov, J. Suarez Gonzalez

Universiteit Antwerpen, Antwerpen, Belgium
E.A. De Wolf, D. Di Croce, X. Janssen, J. Lauwers, M. Van De Klundert, H. Van Haevermaet, P. Van Mechelen, N. Van Remortel

Vrije Universiteit Brussel, Brussel, Belgium
S. Abu Zeid, F. Blekman, J. D'Hondt, I. De Bruyn, J. De Clercq, K. Deroover, G. Flouris, D. Lontkovskyi, S. Lowette, I. Marchesini, S. Moortgat, L. Moreels, Q. Python, K. Skovpen, S. Tavernier, W. Van Doninck, P. Van Mulders, I. Van Parijs

Université Libre de Bruxelles, Bruxelles, Belgium
D. Beghin, B. Bilin, H. Brun, B. Clerbaux, G. De Lentdecker, H. Delannoy, B. Dorney, G. Fasanella, L. Favart, R. Goldouzian, A. Grebenyuk, A.K. Kalsi, T. Lenzi, J. Luetic, T. Maerschalk, A. Marinov, T. Seva, E. Starling, C. Vander Velde, P. Vanlaer, D. Vannerom, R. Yonamine, F. Zenoni

Ghent University, Ghent, Belgium
T. Cornelis, D. Dobur, A. Fagot, M. Gul, I. Khvastunov[2], D. Poyraz, C. Roskas, S. Salva, D. Trocino, M. Tytgat, W. Verbeke, M. Vit, N. Zaganidis

Université Catholique de Louvain, Louvain-la-Neuve, Belgium
H. Bakhshiansohi, O. Bondu, S. Brochet, G. Bruno, C. Caputo, A. Caudron, P. David, S. De Visscher, C. Delaere, M. Delcourt, B. Francois, A. Giammanco, M. Komm, G. Krintiras, V. Lemaitre, A. Magitteri, A. Mertens, M. Musich, K. Piotrzkowski, L. Quertenmont, A. Saggio, M. Vidal Marono, S. Wertz, J. Zobec

Centro Brasileiro de Pesquisas Fisicas, Rio de Janeiro, Brazil
W.L. Aldá Júnior, F.L. Alves, G.A. Alves, L. Brito, G. Correia Silva, C. Hensel, A. Moraes, M.E. Pol, P. Rebello Teles

Universidade do Estado do Rio de Janeiro, Rio de Janeiro, Brazil
E. Belchior Batista Das Chagas, W. Carvalho, J. Chinellato[3], E. Coelho, E.M. Da Costa, G.G. Da Silveira[4], D. De Jesus Damiao, S. Fonseca De Souza, L.M. Huertas Guativa, H. Malbouisson, M. Melo De Almeida, C. Mora Herrera, L. Mundim, H. Nogima, L.J. Sanchez Rosas, A. Santoro, A. Sznajder, M. Thiel, E.J. Tonelli Manganote[3], F. Torres Da Silva De Araujo, A. Vilela Pereira

Universidade Estadual Paulista [a], Universidade Federal do ABC [b], São Paulo, Brazil
S. Ahuja[a], C.A. Bernardes[a], T.R. Fernandez Perez Tomei[a], E.M. Gregores[b], P.G. Mercadante[b], S.F. Novaes[a], Sandra S. Padula[a], D. Romero Abad[b], J.C. Ruiz Vargas[a]

Institute for Nuclear Research and Nuclear Energy, Bulgarian Academy of Sciences, Sofia, Bulgaria
A. Aleksandrov, R. Hadjiiska, P. Iaydjiev, M. Misheva, M. Rodozov, M. Shopova, G. Sultanov

University of Sofia, Sofia, Bulgaria
A. Dimitrov, L. Litov, B. Pavlov, P. Petkov

Beihang University, Beijing, China
W. Fang[5], X. Gao[5], L. Yuan

Institute of High Energy Physics, Beijing, China
M. Ahmad, J.G. Bian, G.M. Chen, H.S. Chen, M. Chen, Y. Chen, C.H. Jiang, D. Leggat, H. Liao, Z. Liu, F. Romeo, S.M. Shaheen, A. Spiezia, J. Tao, C. Wang, Z. Wang, E. Yazgan, H. Zhang, J. Zhao

State Key Laboratory of Nuclear Physics and Technology, Peking University, Beijing, China
Y. Ban, G. Chen, J. Li, Q. Li, S. Liu, Y. Mao, S.J. Qian, D. Wang, Z. Xu, F. Zhang[5]

Tsinghua University, Beijing, China
Y. Wang

Universidad de Los Andes, Bogota, Colombia
C. Avila, A. Cabrera, C.A. Carrillo Montoya, L.F. Chaparro Sierra, C. Florez, C.F. González Hernández, J.D. Ruiz Alvarez, M.A. Segura Delgado

University of Split, Faculty of Electrical Engineering, Mechanical Engineering and Naval Architecture, Split, Croatia
B. Courbon, N. Godinovic, D. Lelas, I. Puljak, P.M. Ribeiro Cipriano, T. Sculac

University of Split, Faculty of Science, Split, Croatia
Z. Antunovic, M. Kovac

Institute Rudjer Boskovic, Zagreb, Croatia
V. Brigljevic, D. Ferencek, K. Kadija, B. Mesic, A. Starodumov[6], T. Susa

University of Cyprus, Nicosia, Cyprus
M.W. Ather, A. Attikis, G. Mavromanolakis, J. Mousa, C. Nicolaou, F. Ptochos, P.A. Razis, H. Rykaczewski

Charles University, Prague, Czech Republic
M. Finger[7], M. Finger Jr.[7]

Universidad San Francisco de Quito, Quito, Ecuador
E. Carrera Jarrin

Academy of Scientific Research and Technology of the Arab Republic of Egypt, Egyptian Network of High Energy Physics, Cairo, Egypt
A. Mohamed[8], Y. Mohammed[9], E. Salama[10,11]

National Institute of Chemical Physics and Biophysics, Tallinn, Estonia
S. Bhowmik, R.K. Dewanjee, M. Kadastik, L. Perrini, M. Raidal, C. Veelken

Department of Physics, University of Helsinki, Helsinki, Finland
P. Eerola, H. Kirschenmann, J. Pekkanen, M. Voutilainen

Helsinki Institute of Physics, Helsinki, Finland
J. Havukainen, J.K. Heikkilä, T. Järvinen, V. Karimäki, R. Kinnunen, T. Lampén, K. Lassila-Perini, S. Laurila, S. Lehti, T. Lindén, P. Luukka, T. Mäenpää, H. Siikonen, E. Tuominen, J. Tuominiemi

Lappeenranta University of Technology, Lappeenranta, Finland
T. Tuuva

IRFU, CEA, Université Paris-Saclay, Gif-sur-Yvette, France
A. Aggarwal, M. Besancon, F. Couderc, M. Dejardin, D. Denegri, J.L. Faure, F. Ferri, S. Ganjour, S. Ghosh, A. Givernaud, P. Gras, G. Hamel de Monchenault, P. Jarry, C. Leloup, E. Locci, M. Machet, J. Malcles, G. Negro, J. Rander, A. Rosowsky, M.Ö. Sahin, M. Titov

Laboratoire Leprince-Ringuet, Ecole polytechnique, CNRS/IN2P3, Université Paris-Saclay, Palaiseau, France
A. Abdulsalam[12], C. Amendola, I. Antropov, S. Baffioni, F. Beaudette, P. Busson, L. Cadamuro, C. Charlot, R. Granier de Cassagnac, M. Jo, I. Kucher, S. Lisniak, A. Lobanov, J. Martin Blanco, M. Nguyen, C. Ochando, G. Ortona, P. Paganini, P. Pigard, R. Salerno, J.B. Sauvan, Y. Sirois, A.G. Stahl Leiton, T. Strebler, Y. Yilmaz, A. Zabi, A. Zghiche

Université de Strasbourg, CNRS, IPHC UMR 7178, F-67000 Strasbourg, France
J.-L. Agram[13], J. Andrea, D. Bloch, J.-M. Brom, M. Buttignol, E.C. Chabert, N. Chanon, C. Collard, E. Conte[13], X. Coubez, F. Drouhin[13], J.-C. Fontaine[13], D. Gelé, U. Goerlach, M. Jansová, P. Juillot, A.-C. Le Bihan, N. Tonon, P. Van Hove

Centre de Calcul de l'Institut National de Physique Nucleaire et de Physique des Particules, CNRS/IN2P3, Villeurbanne, France
S. Gadrat

Université de Lyon, Université Claude Bernard Lyon 1, CNRS-IN2P3, Institut de Physique Nucléaire de Lyon, Villeurbanne, France
S. Beauceron, C. Bernet, G. Boudoul, R. Chierici, D. Contardo, P. Depasse, H. El Mamouni, J. Fay, L. Finco, S. Gascon, M. Gouzevitch, G. Grenier, B. Ille, F. Lagarde, I.B. Laktineh, M. Lethuillier, L. Mirabito, A.L. Pequegnot, S. Perries, A. Popov[14], V. Sordini, M. Vander Donckt, S. Viret, S. Zhang

Georgian Technical University, Tbilisi, Georgia
A. Khvedelidze[7]

Tbilisi State University, Tbilisi, Georgia
Z. Tsamalaidze[7]

RWTH Aachen University, I. Physikalisches Institut, Aachen, Germany
C. Autermann, L. Feld, M.K. Kiesel, K. Klein, M. Lipinski, M. Preuten, C. Schomakers, J. Schulz, M. Teroerde, B. Wittmer, V. Zhukov[14]

RWTH Aachen University, III. Physikalisches Institut A, Aachen, Germany
A. Albert, D. Duchardt, M. Endres, M. Erdmann, S. Erdweg, T. Esch, R. Fischer, A. Güth, T. Hebbeker, C. Heidemann, K. Hoepfner, S. Knutzen, M. Merschmeyer, A. Meyer, P. Millet, S. Mukherjee, T. Pook, M. Radziej, H. Reithler, M. Rieger, F. Scheuch, D. Teyssier, S. Thüer

RWTH Aachen University, III. Physikalisches Institut B, Aachen, Germany
G. Flügge, B. Kargoll, T. Kress, A. Künsken, T. Müller, A. Nehrkorn, A. Nowack, C. Pistone, O. Pooth, A. Stahl[15]

Deutsches Elektronen-Synchrotron, Hamburg, Germany
M. Aldaya Martin, T. Arndt, C. Asawatangtrakuldee, K. Beernaert, O. Behnke, U. Behrens, A. Bermúdez Martínez, A.A. Bin Anuar, K. Borras[16], V. Botta, A. Campbell, P. Connor, C. Contreras-Campana, F. Costanza, C. Diez Pardos, G. Eckerlin, D. Eckstein, T. Eichhorn, E. Eren, E. Gallo[17], J. Garay Garcia, A. Geiser, J.M. Grados Luyando, A. Grohsjean, P. Gunnellini, M. Guthoff, A. Harb, J. Hauk, M. Hempel[18], H. Jung, M. Kasemann, J. Keaveney, C. Kleinwort, I. Korol, D. Krücker, W. Lange, A. Lelek, T. Lenz, K. Lipka, W. Lohmann[18], R. Mankel, I.-A. Melzer-Pellmann, A.B. Meyer, M. Missiroli, G. Mittag, J. Mnich, A. Mussgiller, E. Ntomari, D. Pitzl, A. Raspereza, M. Savitskyi, P. Saxena, R. Shevchenko, N. Stefaniuk, G.P. Van Onsem, R. Walsh, Y. Wen, K. Wichmann, C. Wissing, O. Zenaiev

University of Hamburg, Hamburg, Germany
R. Aggleton, S. Bein, V. Blobel, M. Centis Vignali, T. Dreyer, E. Garutti, D. Gonzalez, J. Haller, A. Hinzmann, M. Hoffmann, A. Karavdina, R. Klanner, R. Kogler, N. Kovalchuk, S. Kurz, D. Marconi, M. Meyer, M. Niedziela, D. Nowatschin, F. Pantaleo[15], T. Peiffer, A. Perieanu, C. Scharf, P. Schleper, A. Schmidt, S. Schumann, J. Schwandt, J. Sonneveld, H. Stadie, G. Steinbrück, F.M. Stober, M. Stöver, H. Tholen, D. Troendle, E. Usai, A. Vanhoefer, B. Vormwald

Institut für Experimentelle Teilchenphysik, Karlsruhe, Germany
M. Akbiyik, C. Barth, M. Baselga, S. Baur, E. Butz, R. Caspart, T. Chwalek, F. Colombo, W. De Boer, A. Dierlamm, N. Faltermann, B. Freund, R. Friese, M. Giffels, M.A. Harrendorf, F. Hartmann[15], S.M. Heindl, U. Husemann, F. Kassel[15], S. Kudella, H. Mildner, M.U. Mozer, Th. Müller, M. Plagge, G. Quast, K. Rabbertz, M. Schröder, I. Shvetsov, G. Sieber, H.J. Simonis, R. Ulrich, S. Wayand, M. Weber, T. Weiler, S. Williamson, C. Wöhrmann, R. Wolf

Institute of Nuclear and Particle Physics (INPP), NCSR Demokritos, Aghia Paraskevi, Greece
G. Anagnostou, G. Daskalakis, T. Geralis, A. Kyriakis, D. Loukas, I. Topsis-Giotis

National and Kapodistrian University of Athens, Athens, Greece
G. Karathanasis, S. Kesisoglou, A. Panagiotou, N. Saoulidou, E. Tziaferi

National Technical University of Athens, Athens, Greece
K. Kousouris

University of Ioánnina, Ioánnina, Greece
I. Evangelou, C. Foudas, P. Gianneios, P. Katsoulis, P. Kokkas, S. Mallios, N. Manthos, I. Papadopoulos, E. Paradas, J. Strologas, F.A. Triantis, D. Tsitsonis

MTA-ELTE Lendület CMS Particle and Nuclear Physics Group, Eötvös Loránd University, Budapest, Hungary
M. Csanad, N. Filipovic, G. Pasztor, O. Surányi, G.I. Veres[19]

Wigner Research Centre for Physics, Budapest, Hungary
G. Bencze, C. Hajdu, D. Horvath[20], Á. Hunyadi, F. Sikler, V. Veszpremi, G. Vesztergombi[19]

Institute of Nuclear Research ATOMKI, Debrecen, Hungary
N. Beni, S. Czellar, J. Karancsi[21], A. Makovec, J. Molnar, Z. Szillasi

Institute of Physics, University of Debrecen, Debrecen, Hungary
M. Bartók[19], P. Raics, Z.L. Trocsanyi, B. Ujvari

Indian Institute of Science (IISc), Bangalore, India
S. Choudhury, J.R. Komaragiri

National Institute of Science Education and Research, Bhubaneswar, India
S. Bahinipati[22], P. Mal, K. Mandal, A. Nayak[23], D.K. Sahoo[22], N. Sahoo, S.K. Swain

Panjab University, Chandigarh, India
S. Bansal, S.B. Beri, V. Bhatnagar, R. Chawla, N. Dhingra, A. Kaur, M. Kaur, S. Kaur, R. Kumar, P. Kumari, A. Mehta, J.B. Singh, G. Walia

University of Delhi, Delhi, India
A. Bhardwaj, S. Chauhan, B.C. Choudhary, R.B. Garg, S. Keshri, A. Kumar, Ashok Kumar, S. Malhotra, M. Naimuddin, K. Ranjan, Aashaq Shah, R. Sharma

Saha Institute of Nuclear Physics, HBNI, Kolkata, India
R. Bhardwaj[24], R. Bhattacharya, S. Bhattacharya, U. Bhawandeep[24], D. Bhowmik, S. Dey, S. Dutt[24], S. Dutta, S. Ghosh, N. Majumdar, A. Modak, K. Mondal, S. Mukhopadhyay, S. Nandan, A. Purohit, P.K. Rout, A. Roy, S. Roy Chowdhury, S. Sarkar, M. Sharan, B. Singh, S. Thakur[24]

Indian Institute of Technology Madras, Madras, India
P.K. Behera

Bhabha Atomic Research Centre, Mumbai, India
R. Chudasama, D. Dutta, V. Jha, V. Kumar, A.K. Mohanty[15], P.K. Netrakanti, L.M. Pant, P. Shukla, A. Topkar

Tata Institute of Fundamental Research-A, Mumbai, India
T. Aziz, S. Dugad, B. Mahakud, S. Mitra, G.B. Mohanty, N. Sur, B. Sutar

Tata Institute of Fundamental Research-B, Mumbai, India
S. Banerjee, S. Bhattacharya, S. Chatterjee, P. Das, M. Guchait, Sa. Jain, S. Kumar, M. Maity[25], G. Majumder, K. Mazumdar, T. Sarkar[25], N. Wickramage[26]

Indian Institute of Science Education and Research (IISER), Pune, India
S. Chauhan, S. Dube, V. Hegde, A. Kapoor, K. Kothekar, S. Pandey, A. Rane, S. Sharma

Institute for Research in Fundamental Sciences (IPM), Tehran, Iran
S. Chenarani[27], E. Eskandari Tadavani, S.M. Etesami[27], M. Khakzad, M. Mohammadi Najafabadi, M. Naseri, S. Paktinat Mehdiabadi[28], F. Rezaei Hosseinabadi, B. Safarzadeh[29], M. Zeinali

University College Dublin, Dublin, Ireland
M. Felcini, M. Grunewald

INFN Sezione di Bari [a], Università di Bari [b], Politecnico di Bari [c], Bari, Italy
M. Abbrescia[a,b], C. Calabria[a,b], A. Colaleo[a], D. Creanza[a,c], L. Cristella[a,b], N. De Filippis[a,c], M. De Palma[a,b], F. Errico[a,b], L. Fiore[a], G. Iaselli[a,c], S. Lezki[a,b], G. Maggi[a,c], M. Maggi[a], G. Miniello[a,b], S. My[a,b], S. Nuzzo[a,b], A. Pompili[a,b], G. Pugliese[a,c], R. Radogna[a], A. Ranieri[a], G. Selvaggi[a,b], A. Sharma[a], L. Silvestris[a,15], R. Venditti[a], P. Verwilligen[a]

INFN Sezione di Bologna [a], Università di Bologna [b], Bologna, Italy
G. Abbiendi[a], C. Battilana[a,b], D. Bonacorsi[a,b], L. Borgonovi[a,b], S. Braibant-Giacomelli[a,b], R. Campanini[a,b], P. Capiluppi[a,b], A. Castro[a,b], F.R. Cavallo[a], S.S. Chhibra[a,b], G. Codispoti[a,b], M. Cuffiani[a,b], G.M. Dallavalle[a], F. Fabbri[a], A. Fanfani[a,b], D. Fasanella[a,b], P. Giacomelli[a], C. Grandi[a], L. Guiducci[a,b], F. Iemmi, S. Marcellini[a], G. Masetti[a], A. Montanari[a], F.L. Navarria[a,b], A. Perrotta[a], A.M. Rossi[a,b], T. Rovelli[a,b], G.P. Siroli[a,b], N. Tosi[a]

INFN Sezione di Catania [a]**, Università di Catania** [b]**, Catania, Italy**
S. Albergo[a,b], S. Costa[a,b], A. Di Mattia[a], F. Giordano[a,b], R. Potenza[a,b], A. Tricomi[a,b], C. Tuve[a,b]

INFN Sezione di Firenze [a]**, Università di Firenze** [b]**, Firenze, Italy**
G. Barbagli[a], K. Chatterjee[a,b], V. Ciulli[a,b], C. Civinini[a], R. D'Alessandro[a,b], E. Focardi[a,b], P. Lenzi[a,b], M. Meschini[a], S. Paoletti[a], L. Russo[a,30], G. Sguazzoni[a], D. Strom[a], L. Viliani[a]

INFN Laboratori Nazionali di Frascati, Frascati, Italy
L. Benussi, S. Bianco, F. Fabbri, D. Piccolo, F. Primavera[15]

INFN Sezione di Genova [a]**, Università di Genova** [b]**, Genova, Italy**
V. Calvelli[a,b], F. Ferro[a], F. Ravera[a,b], E. Robutti[a], S. Tosi[a,b]

INFN Sezione di Milano-Bicocca [a]**, Università di Milano-Bicocca** [b]**, Milano, Italy**
A. Benaglia[a], A. Beschi[b], L. Brianza[a,b], F. Brivio[a,b], V. Ciriolo[a,b,15], M.E. Dinardo[a,b], S. Fiorendi[a,b], S. Gennai[a], A. Ghezzi[a,b], P. Govoni[a,b], M. Malberti[a,b], S. Malvezzi[a], R.A. Manzoni[a,b], D. Menasce[a], L. Moroni[a], M. Paganoni[a,b], K. Pauwels[a,b], D. Pedrini[a], S. Pigazzini[a,b,31], S. Ragazzi[a,b], T. Tabarelli de Fatis[a,b]

INFN Sezione di Napoli [a]**, Università di Napoli 'Federico II'** [b]**, Napoli, Italy, Università della Basilicata** [c]**, Potenza, Italy, Università G. Marconi** [d]**, Roma, Italy**
S. Buontempo[a], N. Cavallo[a,c], S. Di Guida[a,d,15], F. Fabozzi[a,c], F. Fienga[a,b], A.O.M. Iorio[a,b], W.A. Khan[a], L. Lista[a], S. Meola[a,d,15], P. Paolucci[a,15], C. Sciacca[a,b], F. Thyssen[a]

INFN Sezione di Padova [a]**, Università di Padova** [b]**, Padova, Italy, Università di Trento** [c]**, Trento, Italy**
P. Azzi[a], N. Bacchetta[a], L. Benato[a,b], D. Bisello[a,b], A. Boletti[a,b], R. Carlin[a,b], A. Carvalho Antunes De Oliveira[a,b], P. Checchia[a], M. Dall'Osso[a,b], P. De Castro Manzano[a], T. Dorigo[a], U. Dosselli[a], F. Gasparini[a,b], U. Gasparini[a,b], A. Gozzelino[a], S. Lacaprara[a], P. Lujan, M. Margoni[a,b], A.T. Meneguzzo[a,b], N. Pozzobon[a,b], P. Ronchese[a,b], R. Rossin[a,b], F. Simonetto[a,b], A. Tiko, E. Torassa[a], M. Zanetti[a,b], P. Zotto[a,b]

INFN Sezione di Pavia [a]**, Università di Pavia** [b]**, Pavia, Italy**
A. Braghieri[a], A. Magnani[a], P. Montagna[a,b], S.P. Ratti[a,b], V. Re[a], M. Ressegotti[a,b], C. Riccardi[a,b], P. Salvini[a], I. Vai[a,b], P. Vitulo[a,b]

INFN Sezione di Perugia [a]**, Università di Perugia** [b]**, Perugia, Italy**
L. Alunni Solestizi[a,b], M. Biasini[a,b], G.M. Bilei[a], C. Cecchi[a,b], D. Ciangottini[a,b], L. Fanò[a,b], P. Lariccia[a,b], R. Leonardi[a,b], E. Manoni[a], G. Mantovani[a,b], V. Mariani[a,b], M. Menichelli[a], A. Rossi[a,b], A. Santocchia[a,b], D. Spiga[a]

INFN Sezione di Pisa [a]**, Università di Pisa** [b]**, Scuola Normale Superiore di Pisa** [c]**, Pisa, Italy**
K. Androsov[a], P. Azzurri[a,15], G. Bagliesi[a], L. Bianchini[a], T. Boccali[a], L. Borrello, R. Castaldi[a], M.A. Ciocci[a,b], R. Dell'Orso[a], G. Fedi[a], L. Giannini[a,c], A. Giassi[a], M.T. Grippo[a,30], F. Ligabue[a,c], T. Lomtadze[a], E. Manca[a,c], G. Mandorli[a,c], A. Messineo[a,b], F. Palla[a], A. Rizzi[a,b], A. Savoy-Navarro[a,32], P. Spagnolo[a], R. Tenchini[a], G. Tonelli[a,b], A. Venturi[a], P.G. Verdini[a]

INFN Sezione di Roma [a]**, Sapienza Università di Roma** [b]**, Rome, Italy**
L. Barone[a,b], F. Cavallari[a], M. Cipriani[a,b], N. Daci[a], D. Del Re[a,b], E. Di Marco[a,b], M. Diemoz[a], S. Gelli[a,b], E. Longo[a,b], F. Margaroli[a,b], B. Marzocchi[a,b], P. Meridiani[a], G. Organtini[a,b], R. Paramatti[a,b], F. Preiato[a,b], S. Rahatlou[a,b], C. Rovelli[a], F. Santanastasio[a,b]

INFN Sezione di Torino [a]**, Università di Torino** [b]**, Torino, Italy, Università del Piemonte Orientale** [c]**, Novara, Italy**
N. Amapane[a,b], R. Arcidiacono[a,c], S. Argiro[a,b], M. Arneodo[a,c], N. Bartosik[a], R. Bellan[a,b],

C. Biino[a], N. Cartiglia[a], F. Cenna[a,b], M. Costa[a,b], R. Covarelli[a,b], A. Degano[a,b], N. Demaria[a], B. Kiani[a,b], C. Mariotti[a], S. Maselli[a], E. Migliore[a,b], V. Monaco[a,b], E. Monteil[a,b], M. Monteno[a], M.M. Obertino[a,b], L. Pacher[a,b], N. Pastrone[a], M. Pelliccioni[a], G.L. Pinna Angioni[a,b], A. Romero[a,b], M. Ruspa[a,c], R. Sacchi[a,b], K. Shchelina[a,b], V. Sola[a], A. Solano[a,b], A. Staiano[a], P. Traczyk[a,b]

INFN Sezione di Trieste [a], Università di Trieste [b], Trieste, Italy
S. Belforte[a], M. Casarsa[a], F. Cossutti[a], G. Della Ricca[a,b], A. Zanetti[a]

Kyungpook National University
D.H. Kim, G.N. Kim, M.S. Kim, J. Lee, S. Lee, S.W. Lee, C.S. Moon, Y.D. Oh, S. Sekmen, D.C. Son, Y.C. Yang

Chonnam National University, Institute for Universe and Elementary Particles, Kwangju, Korea
H. Kim, D.H. Moon, G. Oh

Hanyang University, Seoul, Korea
J.A. Brochero Cifuentes, J. Goh, T.J. Kim

Korea University, Seoul, Korea
S. Cho, S. Choi, Y. Go, D. Gyun, S. Ha, B. Hong, Y. Jo, Y. Kim, K. Lee, K.S. Lee, S. Lee, J. Lim, S.K. Park, Y. Roh

Seoul National University, Seoul, Korea
J. Almond, J. Kim, J.S. Kim, H. Lee, K. Lee, K. Nam, S.B. Oh, B.C. Radburn-Smith, S.h. Seo, U.K. Yang, H.D. Yoo, G.B. Yu

University of Seoul, Seoul, Korea
H. Kim, J.H. Kim, J.S.H. Lee, I.C. Park

Sungkyunkwan University, Suwon, Korea
Y. Choi, C. Hwang, J. Lee, I. Yu

Vilnius University, Vilnius, Lithuania
V. Dudenas, A. Juodagalvis, J. Vaitkus

National Centre for Particle Physics, Universiti Malaya, Kuala Lumpur, Malaysia
I. Ahmed, Z.A. Ibrahim, M.A.B. Md Ali[33], F. Mohamad Idris[34], W.A.T. Wan Abdullah, M.N. Yusli, Z. Zolkapli

Centro de Investigacion y de Estudios Avanzados del IPN, Mexico City, Mexico
Duran-Osuna, M. C., H. Castilla-Valdez, E. De La Cruz-Burelo, Ramirez-Sanchez, G., I. Heredia-De La Cruz[35], Rabadan-Trejo, R. I., R. Lopez-Fernandez, J. Mejia Guisao, Reyes-Almanza, R, A. Sanchez-Hernandez

Universidad Iberoamericana, Mexico City, Mexico
S. Carrillo Moreno, C. Oropeza Barrera, F. Vazquez Valencia

Benemerita Universidad Autonoma de Puebla, Puebla, Mexico
J. Eysermans, I. Pedraza, H.A. Salazar Ibarguen, C. Uribe Estrada

Universidad Autónoma de San Luis Potosí, San Luis Potosí, Mexico
A. Morelos Pineda

University of Auckland, Auckland, New Zealand
D. Krofcheck

University of Canterbury, Christchurch, New Zealand
P.H. Butler

National Centre for Physics, Quaid-I-Azam University, Islamabad, Pakistan
A. Ahmad, M. Ahmad, Q. Hassan, H.R. Hoorani, A. Saddique, M.A. Shah, M. Shoaib, M. Waqas

National Centre for Nuclear Research, Swierk, Poland
H. Bialkowska, M. Bluj, B. Boimska, T. Frueboes, M. Górski, M. Kazana, K. Nawrocki, M. Szleper, P. Zalewski

Institute of Experimental Physics, Faculty of Physics, University of Warsaw, Warsaw, Poland
K. Bunkowski, A. Byszuk[36], K. Doroba, A. Kalinowski, M. Konecki, J. Krolikowski, M. Misiura, M. Olszewski, A. Pyskir, M. Walczak

Laboratório de Instrumentação e Física Experimental de Partículas, Lisboa, Portugal
P. Bargassa, C. Beirão Da Cruz E Silva, A. Di Francesco, P. Faccioli, B. Galinhas, M. Gallinaro, J. Hollar, N. Leonardo, L. Lloret Iglesias, M.V. Nemallapudi, J. Seixas, G. Strong, O. Toldaiev, D. Vadruccio, J. Varela

Joint Institute for Nuclear Research, Dubna, Russia
S. Afanasiev, P. Bunin, M. Gavrilenko, I. Golutvin, I. Gorbunov, A. Kamenev, V. Karjavin, A. Lanev, A. Malakhov, V. Matveev[37,38], P. Moisenz, V. Palichik, V. Perelygin, S. Shmatov, S. Shulha, N. Skatchkov, V. Smirnov, N. Voytishin, A. Zarubin

Petersburg Nuclear Physics Institute, Gatchina (St. Petersburg), Russia
Y. Ivanov, V. Kim[39], E. Kuznetsova[40], P. Levchenko, V. Murzin, V. Oreshkin, I. Smirnov, D. Sosnov, V. Sulimov, L. Uvarov, S. Vavilov, A. Vorobyev

Institute for Nuclear Research, Moscow, Russia
Yu. Andreev, A. Dermenev, S. Gninenko, N. Golubev, A. Karneyeu, M. Kirsanov, N. Krasnikov, A. Pashenkov, D. Tlisov, A. Toropin

Institute for Theoretical and Experimental Physics, Moscow, Russia
V. Epshteyn, V. Gavrilov, N. Lychkovskaya, V. Popov, I. Pozdnyakov, G. Safronov, A. Spiridonov, A. Stepennov, V. Stolin, M. Toms, E. Vlasov, A. Zhokin

Moscow Institute of Physics and Technology, Moscow, Russia
T. Aushev, A. Bylinkin[38]

National Research Nuclear University 'Moscow Engineering Physics Institute' (MEPhI), Moscow, Russia
R. Chistov[41], M. Danilov[41], P. Parygin, D. Philippov, S. Polikarpov, E. Tarkovskii

P.N. Lebedev Physical Institute, Moscow, Russia
V. Andreev, M. Azarkin[38], I. Dremin[38], M. Kirakosyan[38], S.V. Rusakov, A. Terkulov

Skobeltsyn Institute of Nuclear Physics, Lomonosov Moscow State University, Moscow, Russia
A. Baskakov, A. Belyaev, E. Boos, V. Bunichev, M. Dubinin[42], L. Dudko, A. Ershov, V. Klyukhin, O. Kodolova, I. Lokhtin, I. Miagkov, S. Obraztsov, S. Petrushanko, V. Savrin, A. Snigirev

Novosibirsk State University (NSU), Novosibirsk, Russia
V. Blinov[43], D. Shtol[43], Y. Skovpen[43]

State Research Center of Russian Federation, Institute for High Energy Physics of NRC &quot, Kurchatov Institute&quot, , Protvino, Russia
I. Azhgirey, I. Bayshev, S. Bitioukov, D. Elumakhov, A. Godizov, V. Kachanov, A. Kalinin, D. Konstantinov, P. Mandrik, V. Petrov, R. Ryutin, A. Sobol, S. Troshin, N. Tyurin, A. Uzunian, A. Volkov

University of Belgrade, Faculty of Physics and Vinca Institute of Nuclear Sciences, Belgrade, Serbia
P. Adzic[44], P. Cirkovic, D. Devetak, M. Dordevic, J. Milosevic

Centro de Investigaciones Energéticas Medioambientales y Tecnológicas (CIEMAT), Madrid, Spain
J. Alcaraz Maestre, A. Álvarez Fernández, I. Bachiller, M. Barrio Luna, M. Cerrada, N. Colino, B. De La Cruz, A. Delgado Peris, C. Fernandez Bedoya, J.P. Fernández Ramos, J. Flix, M.C. Fouz, O. Gonzalez Lopez, S. Goy Lopez, J.M. Hernandez, M.I. Josa, D. Moran, A. Pérez-Calero Yzquierdo, J. Puerta Pelayo, I. Redondo, L. Romero, M.S. Soares, A. Triossi

Universidad Autónoma de Madrid, Madrid, Spain
C. Albajar, J.F. de Trocóniz

Universidad de Oviedo, Oviedo, Spain
J. Cuevas, C. Erice, J. Fernandez Menendez, I. Gonzalez Caballero, J.R. González Fernández, E. Palencia Cortezon, S. Sanchez Cruz, P. Vischia, J.M. Vizan Garcia

Instituto de Física de Cantabria (IFCA), CSIC-Universidad de Cantabria, Santander, Spain
I.J. Cabrillo, A. Calderon, B. Chazin Quero, E. Curras, J. Duarte Campderros, M. Fernandez, P.J. Fernández Manteca, A. García Alonso, J. Garcia-Ferrero, G. Gomez, A. Lopez Virto, J. Marco, C. Martinez Rivero, P. Martinez Ruiz del Arbol, F. Matorras, J. Piedra Gomez, C. Prieels, T. Rodrigo, A. Ruiz-Jimeno, L. Scodellaro, N. Trevisani, I. Vila, R. Vilar Cortabitarte

CERN, European Organization for Nuclear Research, Geneva, Switzerland
D. Abbaneo, B. Akgun, E. Auffray, P. Baillon, A.H. Ball, D. Barney, J. Bendavid, M. Bianco, A. Bocci, C. Botta, T. Camporesi, R. Castello, M. Cepeda, G. Cerminara, E. Chapon, Y. Chen, D. d'Enterria, A. Dabrowski, V. Daponte, A. David, M. De Gruttola, A. De Roeck, N. Deelen, M. Dobson, T. du Pree, M. Dünser, N. Dupont, A. Elliott-Peisert, P. Everaerts, F. Fallavollita, G. Franzoni, J. Fulcher, W. Funk, D. Gigi, A. Gilbert, K. Gill, F. Glege, D. Gulhan, J. Hegeman, V. Innocente, A. Jafari, P. Janot, O. Karacheban[18], J. Kieseler, V. Knünz, A. Kornmayer, M.J. Kortelainen, M. Krammer[1], C. Lange, P. Lecoq, C. Lourenço, M.T. Lucchini, L. Malgeri, M. Mannelli, A. Martelli, F. Meijers, J.A. Merlin, S. Mersi, E. Meschi, P. Milenovic[45], F. Moortgat, M. Mulders, H. Neugebauer, J. Ngadiuba, S. Orfanelli, L. Orsini, L. Pape, E. Perez, M. Peruzzi, A. Petrilli, G. Petrucciani, A. Pfeiffer, M. Pierini, F.M. Pitters, D. Rabady, A. Racz, T. Reis, G. Rolandi[46], M. Rovere, H. Sakulin, C. Schäfer, C. Schwick, M. Seidel, M. Selvaggi, A. Sharma, P. Silva, P. Sphicas[47], A. Stakia, J. Steggemann, M. Stoye, M. Tosi, D. Treille, A. Tsirou, V. Veckalns[48], M. Verweij, W.D. Zeuner

Paul Scherrer Institut, Villigen, Switzerland
W. Bertl[†], L. Caminada[49], K. Deiters, W. Erdmann, R. Horisberger, Q. Ingram, H.C. Kaestli, D. Kotlinski, U. Langenegger, T. Rohe, S.A. Wiederkehr

ETH Zurich - Institute for Particle Physics and Astrophysics (IPA), Zurich, Switzerland
M. Backhaus, L. Bäni, P. Berger, B. Casal, G. Dissertori, M. Dittmar, M. Donegà, C. Dorfer, C. Grab, C. Heidegger, D. Hits, J. Hoss, G. Kasieczka, T. Klijnsma, W. Lustermann, B. Mangano, M. Marionneau, M.T. Meinhard, D. Meister, F. Micheli, P. Musella, F. Nessi-Tedaldi, F. Pandolfi,

J. Pata, F. Pauss, G. Perrin, L. Perrozzi, M. Quittnat, M. Reichmann, D.A. Sanz Becerra, M. Schönenberger, L. Shchutska, V.R. Tavolaro, K. Theofilatos, M.L. Vesterbacka Olsson, R. Wallny, D.H. Zhu

Universität Zürich, Zurich, Switzerland
T.K. Aarrestad, C. Amsler[50], M.F. Canelli, A. De Cosa, R. Del Burgo, S. Donato, C. Galloni, T. Hreus, B. Kilminster, D. Pinna, G. Rauco, P. Robmann, D. Salerno, K. Schweiger, C. Seitz, Y. Takahashi, A. Zucchetta

National Central University, Chung-Li, Taiwan
V. Candelise, Y.H. Chang, K.y. Cheng, T.H. Doan, Sh. Jain, R. Khurana, C.M. Kuo, W. Lin, A. Pozdnyakov, C.W. Yeh, S.S. Yu

National Taiwan University (NTU), Taipei, Taiwan
P. Chang, Y. Chao, K.F. Chen, P.H. Chen, F. Fiori, W.-S. Hou, Y. Hsiung, Arun Kumar, Y.F. Liu, R.-S. Lu, E. Paganis, A. Psallidas, A. Steen, J.f. Tsai

Chulalongkorn University, Faculty of Science, Department of Physics, Bangkok, Thailand
B. Asavapibhop, K. Kovitanggoon, G. Singh, N. Srimanobhas

Çukurova University, Physics Department, Science and Art Faculty, Adana, Turkey
A. Bat, F. Boran, S. Cerci[51], S. Damarseckin, Z.S. Demiroglu, C. Dozen, I. Dumanoglu, S. Girgis, G. Gokbulut, Y. Guler, I. Hos[52], E.E. Kangal[53], O. Kara, U. Kiminsu, M. Oglakci, G. Onengut, K. Ozdemir[54], D. Sunar Cerci[51], B. Tali[51], U.G. Tok, H. Topakli[55], S. Turkcapar, I.S. Zorbakir, C. Zorbilmez

Middle East Technical University, Physics Department, Ankara, Turkey
G. Karapinar[56], K. Ocalan[57], M. Yalvac, M. Zeyrek

Bogazici University, Istanbul, Turkey
E. Gülmez, M. Kaya[58], O. Kaya[59], S. Tekten, E.A. Yetkin[60]

Istanbul Technical University, Istanbul, Turkey
M.N. Agaras, S. Atay, A. Cakir, K. Cankocak, Y. Komurcu

Institute for Scintillation Materials of National Academy of Science of Ukraine, Kharkov, Ukraine
B. Grynyov

National Scientific Center, Kharkov Institute of Physics and Technology, Kharkov, Ukraine
L. Levchuk

University of Bristol, Bristol, United Kingdom
F. Ball, L. Beck, J.J. Brooke, D. Burns, E. Clement, D. Cussans, O. Davignon, H. Flacher, J. Goldstein, G.P. Heath, H.F. Heath, L. Kreczko, D.M. Newbold[61], S. Paramesvaran, T. Sakuma, S. Seif El Nasr-storey, D. Smith, V.J. Smith

Rutherford Appleton Laboratory, Didcot, United Kingdom
K.W. Bell, A. Belyaev[62], C. Brew, R.M. Brown, L. Calligaris, D. Cieri, D.J.A. Cockerill, J.A. Coughlan, K. Harder, S. Harper, J. Linacre, E. Olaiya, D. Petyt, C.H. Shepherd-Themistocleous, A. Thea, I.R. Tomalin, T. Williams, W.J. Womersley

Imperial College, London, United Kingdom
G. Auzinger, R. Bainbridge, P. Bloch, J. Borg, S. Breeze, O. Buchmuller, A. Bundock, S. Casasso, M. Citron, D. Colling, L. Corpe, P. Dauncey, G. Davies, M. Della Negra, R. Di Maria, Y. Haddad, G. Hall, G. Iles, T. James, R. Lane, C. Laner, L. Lyons, A.-M. Magnan,

S. Malik, L. Mastrolorenzo, T. Matsushita, J. Nash[63], A. Nikitenko[6], V. Palladino, M. Pesaresi, D.M. Raymond, A. Richards, A. Rose, E. Scott, C. Seez, A. Shtipliyski, S. Summers, A. Tapper, K. Uchida, M. Vazquez Acosta[64], T. Virdee[15], N. Wardle, D. Winterbottom, J. Wright, S.C. Zenz

Brunel University, Uxbridge, United Kingdom
J.E. Cole, P.R. Hobson, A. Khan, P. Kyberd, A. Morton, I.D. Reid, L. Teodorescu, S. Zahid

Baylor University, Waco, USA
A. Borzou, K. Call, J. Dittmann, K. Hatakeyama, H. Liu, N. Pastika, C. Smith

Catholic University of America, Washington DC, USA
R. Bartek, A. Dominguez

The University of Alabama, Tuscaloosa, USA
A. Buccilli, S.I. Cooper, C. Henderson, P. Rumerio, C. West

Boston University, Boston, USA
D. Arcaro, A. Avetisyan, T. Bose, D. Gastler, D. Rankin, C. Richardson, J. Rohlf, L. Sulak, D. Zou

Brown University, Providence, USA
G. Benelli, D. Cutts, M. Hadley, J. Hakala, U. Heintz, J.M. Hogan, K.H.M. Kwok, E. Laird, G. Landsberg, J. Lee, Z. Mao, M. Narain, J. Pazzini, S. Piperov, S. Sagir, R. Syarif, D. Yu

University of California, Davis, Davis, USA
R. Band, C. Brainerd, R. Breedon, D. Burns, M. Calderon De La Barca Sanchez, M. Chertok, J. Conway, R. Conway, P.T. Cox, R. Erbacher, C. Flores, G. Funk, W. Ko, R. Lander, C. Mclean, M. Mulhearn, D. Pellett, J. Pilot, S. Shalhout, M. Shi, J. Smith, D. Stolp, D. Taylor, K. Tos, M. Tripathi, Z. Wang

University of California, Los Angeles, USA
M. Bachtis, C. Bravo, R. Cousins, A. Dasgupta, A. Florent, J. Hauser, M. Ignatenko, N. Mccoll, S. Regnard, D. Saltzberg, C. Schnaible, V. Valuev

University of California, Riverside, Riverside, USA
E. Bouvier, K. Burt, R. Clare, J. Ellison, J.W. Gary, S.M.A. Ghiasi Shirazi, G. Hanson, J. Heilman, G. Karapostoli, E. Kennedy, F. Lacroix, O.R. Long, M. Olmedo Negrete, M.I. Paneva, W. Si, L. Wang, H. Wei, S. Wimpenny, B. R. Yates

University of California, San Diego, La Jolla, USA
J.G. Branson, S. Cittolin, M. Derdzinski, R. Gerosa, D. Gilbert, B. Hashemi, A. Holzner, D. Klein, G. Kole, V. Krutelyov, J. Letts, M. Masciovecchio, D. Olivito, S. Padhi, M. Pieri, M. Sani, V. Sharma, S. Simon, M. Tadel, A. Vartak, S. Wasserbaech[65], J. Wood, F. Würthwein, A. Yagil, G. Zevi Della Porta

University of California, Santa Barbara - Department of Physics, Santa Barbara, USA
N. Amin, R. Bhandari, J. Bradmiller-Feld, C. Campagnari, A. Dishaw, V. Dutta, M. Franco Sevilla, L. Gouskos, R. Heller, J. Incandela, A. Ovcharova, H. Qu, J. Richman, D. Stuart, I. Suarez, J. Yoo

California Institute of Technology, Pasadena, USA
D. Anderson, A. Bornheim, J. Bunn, I. Dutta, J.M. Lawhorn, H.B. Newman, T. Q. Nguyen, C. Pena, M. Spiropulu, J.R. Vlimant, R. Wilkinson, S. Xie, Z. Zhang, R.Y. Zhu

Carnegie Mellon University, Pittsburgh, USA
M.B. Andrews, T. Ferguson, T. Mudholkar, M. Paulini, J. Russ, M. Sun, H. Vogel, I. Vorobiev, M. Weinberg

University of Colorado Boulder, Boulder, USA
J.P. Cumalat, W.T. Ford, F. Jensen, A. Johnson, M. Krohn, S. Leontsinis, E. Macdonald, T. Mulholland, K. Stenson, S.R. Wagner

Cornell University, Ithaca, USA
J. Alexander, J. Chaves, Y. Cheng, J. Chu, S. Dittmer, K. Mcdermott, N. Mirman, J.R. Patterson, D. Quach, A. Rinkevicius, A. Ryd, L. Skinnari, L. Soffi, S.M. Tan, Z. Tao, J. Thom, J. Tucker, P. Wittich, M. Zientek

Fermi National Accelerator Laboratory, Batavia, USA
S. Abdullin, M. Albrow, M. Alyari, G. Apollinari, A. Apresyan, A. Apyan, S. Banerjee, L.A.T. Bauerdick, A. Beretvas, J. Berryhill, P.C. Bhat, G. Bolla[†], K. Burkett, J.N. Butler, A. Canepa, G.B. Cerati, H.W.K. Cheung, F. Chlebana, M. Cremonesi, J. Duarte, V.D. Elvira, J. Freeman, Z. Gecse, E. Gottschalk, L. Gray, D. Green, S. Grünendahl, O. Gutsche, J. Hanlon, R.M. Harris, S. Hasegawa, J. Hirschauer, Z. Hu, B. Jayatilaka, S. Jindariani, M. Johnson, U. Joshi, B. Klima, B. Kreis, S. Lammel, D. Lincoln, R. Lipton, M. Liu, T. Liu, R. Lopes De Sá, J. Lykken, K. Maeshima, N. Magini, J.M. Marraffino, D. Mason, P. McBride, P. Merkel, S. Mrenna, S. Nahn, V. O'Dell, K. Pedro, O. Prokofyev, G. Rakness, L. Ristori, B. Schneider, E. Sexton-Kennedy, A. Soha, W.J. Spalding, L. Spiegel, S. Stoynev, J. Strait, N. Strobbe, L. Taylor, S. Tkaczyk, N.V. Tran, L. Uplegger, E.W. Vaandering, C. Vernieri, M. Verzocchi, R. Vidal, M. Wang, H.A. Weber, A. Whitbeck, W. Wu

University of Florida, Gainesville, USA
D. Acosta, P. Avery, P. Bortignon, D. Bourilkov, A. Brinkerhoff, A. Carnes, M. Carver, D. Curry, R.D. Field, I.K. Furic, S.V. Gleyzer, B.M. Joshi, J. Konigsberg, A. Korytov, K. Kotov, P. Ma, K. Matchev, H. Mei, G. Mitselmakher, K. Shi, D. Sperka, N. Terentyev, L. Thomas, J. Wang, S. Wang, J. Yelton

Florida International University, Miami, USA
Y.R. Joshi, S. Linn, P. Markowitz, J.L. Rodriguez

Florida State University, Tallahassee, USA
A. Ackert, T. Adams, A. Askew, S. Hagopian, V. Hagopian, K.F. Johnson, T. Kolberg, G. Martinez, T. Perry, H. Prosper, A. Saha, A. Santra, V. Sharma, R. Yohay

Florida Institute of Technology, Melbourne, USA
M.M. Baarmand, V. Bhopatkar, S. Colafranceschi, M. Hohlmann, D. Noonan, T. Roy, F. Yumiceva

University of Illinois at Chicago (UIC), Chicago, USA
M.R. Adams, L. Apanasevich, D. Berry, R.R. Betts, R. Cavanaugh, X. Chen, O. Evdokimov, C.E. Gerber, D.A. Hangal, D.J. Hofman, K. Jung, J. Kamin, I.D. Sandoval Gonzalez, M.B. Tonjes, H. Trauger, N. Varelas, H. Wang, Z. Wu, J. Zhang

The University of Iowa, Iowa City, USA
B. Bilki[66], W. Clarida, K. Dilsiz[67], S. Durgut, R.P. Gandrajula, M. Haytmyradov, V. Khristenko, J.-P. Merlo, H. Mermerkaya[68], A. Mestvirishvili, A. Moeller, J. Nachtman, H. Ogul[69], Y. Onel, F. Ozok[70], A. Penzo, C. Snyder, E. Tiras, J. Wetzel, K. Yi

Johns Hopkins University, Baltimore, USA
B. Blumenfeld, A. Cocoros, N. Eminizer, D. Fehling, L. Feng, A.V. Gritsan, P. Maksimovic, J. Roskes, U. Sarica, M. Swartz, M. Xiao, C. You

The University of Kansas, Lawrence, USA
A. Al-bataineh, P. Baringer, A. Bean, S. Boren, J. Bowen, J. Castle, S. Khalil, A. Kropivnitskaya, D. Majumder, W. Mcbrayer, M. Murray, C. Rogan, C. Royon, S. Sanders, E. Schmitz, J.D. Tapia Takaki, Q. Wang

Kansas State University, Manhattan, USA
A. Ivanov, K. Kaadze, Y. Maravin, A. Mohammadi, L.K. Saini, N. Skhirtladze

Lawrence Livermore National Laboratory, Livermore, USA
F. Rebassoo, D. Wright

University of Maryland, College Park, USA
A. Baden, O. Baron, A. Belloni, S.C. Eno, Y. Feng, C. Ferraioli, N.J. Hadley, S. Jabeen, G.Y. Jeng, R.G. Kellogg, J. Kunkle, A.C. Mignerey, F. Ricci-Tam, Y.H. Shin, A. Skuja, S.C. Tonwar

Massachusetts Institute of Technology, Cambridge, USA
D. Abercrombie, B. Allen, V. Azzolini, R. Barbieri, A. Baty, G. Bauer, R. Bi, S. Brandt, W. Busza, I.A. Cali, M. D'Alfonso, Z. Demiragli, G. Gomez Ceballos, M. Goncharov, P. Harris, D. Hsu, M. Hu, Y. Iiyama, G.M. Innocenti, M. Klute, D. Kovalskyi, Y.-J. Lee, A. Levin, P.D. Luckey, B. Maier, A.C. Marini, C. Mcginn, C. Mironov, S. Narayanan, X. Niu, C. Paus, C. Roland, G. Roland, J. Salfeld-Nebgen, G.S.F. Stephans, K. Sumorok, K. Tatar, D. Velicanu, J. Wang, T.W. Wang, B. Wyslouch

University of Minnesota, Minneapolis, USA
A.C. Benvenuti, R.M. Chatterjee, A. Evans, P. Hansen, J. Hiltbrand, S. Kalafut, Y. Kubota, Z. Lesko, J. Mans, S. Nourbakhsh, N. Ruckstuhl, R. Rusack, J. Turkewitz, M.A. Wadud

University of Mississippi, Oxford, USA
J.G. Acosta, S. Oliveros

University of Nebraska-Lincoln, Lincoln, USA
E. Avdeeva, K. Bloom, D.R. Claes, C. Fangmeier, F. Golf, R. Gonzalez Suarez, R. Kamalieddin, I. Kravchenko, J. Monroy, J.E. Siado, G.R. Snow, B. Stieger

State University of New York at Buffalo, Buffalo, USA
J. Dolen, A. Godshalk, C. Harrington, I. Iashvili, D. Nguyen, A. Parker, S. Rappoccio, B. Roozbahani

Northeastern University, Boston, USA
G. Alverson, E. Barberis, C. Freer, A. Hortiangtham, A. Massironi, D.M. Morse, T. Orimoto, R. Teixeira De Lima, T. Wamorkar, B. Wang, A. Wisecarver, D. Wood

Northwestern University, Evanston, USA
S. Bhattacharya, O. Charaf, K.A. Hahn, N. Mucia, N. Odell, M.H. Schmitt, K. Sung, M. Trovato, M. Velasco

University of Notre Dame, Notre Dame, USA
R. Bucci, N. Dev, M. Hildreth, K. Hurtado Anampa, C. Jessop, D.J. Karmgard, N. Kellams, K. Lannon, W. Li, N. Loukas, N. Marinelli, F. Meng, C. Mueller, Y. Musienko[37], M. Planer, A. Reinsvold, R. Ruchti, P. Siddireddy, G. Smith, S. Taroni, M. Wayne, A. Wightman, M. Wolf, A. Woodard

The Ohio State University, Columbus, USA
J. Alimena, L. Antonelli, B. Bylsma, L.S. Durkin, S. Flowers, B. Francis, A. Hart, C. Hill, W. Ji, T.Y. Ling, B. Liu, W. Luo, B.L. Winer, H.W. Wulsin

Princeton University, Princeton, USA
S. Cooperstein, O. Driga, P. Elmer, J. Hardenbrook, P. Hebda, S. Higginbotham, A. Kalogeropoulos, D. Lange, J. Luo, D. Marlow, K. Mei, I. Ojalvo, J. Olsen, C. Palmer, P. Piroué, D. Stickland, C. Tully

University of Puerto Rico, Mayaguez, USA
S. Malik, S. Norberg

Purdue University, West Lafayette, USA
A. Barker, V.E. Barnes, S. Das, S. Folgueras, L. Gutay, M. Jones, A.W. Jung, A. Khatiwada, D.H. Miller, N. Neumeister, C.C. Peng, H. Qiu, J.F. Schulte, J. Sun, F. Wang, R. Xiao, W. Xie

Purdue University Northwest, Hammond, USA
T. Cheng, N. Parashar, J. Stupak

Rice University, Houston, USA
Z. Chen, K.M. Ecklund, S. Freed, F.J.M. Geurts, M. Guilbaud, M. Kilpatrick, W. Li, B. Michlin, B.P. Padley, J. Roberts, J. Rorie, W. Shi, Z. Tu, J. Zabel, A. Zhang

University of Rochester, Rochester, USA
A. Bodek, P. de Barbaro, R. Demina, Y.t. Duh, T. Ferbel, M. Galanti, A. Garcia-Bellido, J. Han, O. Hindrichs, A. Khukhunaishvili, K.H. Lo, P. Tan, M. Verzetti

The Rockefeller University, New York, USA
R. Ciesielski, K. Goulianos, C. Mesropian

Rutgers, The State University of New Jersey, Piscataway, USA
A. Agapitos, J.P. Chou, Y. Gershtein, T.A. Gómez Espinosa, E. Halkiadakis, M. Heindl, E. Hughes, S. Kaplan, R. Kunnawalkam Elayavalli, S. Kyriacou, A. Lath, R. Montalvo, K. Nash, M. Osherson, H. Saka, S. Salur, S. Schnetzer, D. Sheffield, S. Somalwar, R. Stone, S. Thomas, P. Thomassen, M. Walker

University of Tennessee, Knoxville, USA
A.G. Delannoy, J. Heideman, G. Riley, K. Rose, S. Spanier, K. Thapa

Texas A&M University, College Station, USA
O. Bouhali[71], A. Castaneda Hernandez[71], A. Celik, M. Dalchenko, M. De Mattia, A. Delgado, S. Dildick, R. Eusebi, J. Gilmore, T. Huang, T. Kamon[72], R. Mueller, Y. Pakhotin, R. Patel, A. Perloff, L. Perniè, D. Rathjens, A. Safonov, A. Tatarinov, K.A. Ulmer

Texas Tech University, Lubbock, USA
N. Akchurin, J. Damgov, F. De Guio, P.R. Dudero, J. Faulkner, E. Gurpinar, S. Kunori, K. Lamichhane, S.W. Lee, T. Mengke, S. Muthumuni, T. Peltola, S. Undleeb, I. Volobouev, Z. Wang

Vanderbilt University, Nashville, USA
S. Greene, A. Gurrola, R. Janjam, W. Johns, C. Maguire, A. Melo, H. Ni, K. Padeken, P. Sheldon, S. Tuo, J. Velkovska, Q. Xu

University of Virginia, Charlottesville, USA
M.W. Arenton, P. Barria, B. Cox, R. Hirosky, M. Joyce, A. Ledovskoy, H. Li, C. Neu, T. Sinthuprasith, Y. Wang, E. Wolfe, F. Xia

Wayne State University, Detroit, USA
R. Harr, P.E. Karchin, N. Poudyal, J. Sturdy, P. Thapa, S. Zaleski

University of Wisconsin - Madison, Madison, WI, USA
M. Brodski, J. Buchanan, C. Caillol, D. Carlsmith, S. Dasu, L. Dodd, S. Duric, B. Gomber, M. Grothe, M. Herndon, A. Hervé, U. Hussain, P. Klabbers, A. Lanaro, A. Levine, K. Long, R. Loveless, V. Rekovic, T. Ruggles, A. Savin, N. Smith, W.H. Smith, N. Woods

†: Deceased
1: Also at Vienna University of Technology, Vienna, Austria
2: Also at IRFU; CEA; Université Paris-Saclay, Gif-sur-Yvette, France
3: Also at Universidade Estadual de Campinas, Campinas, Brazil
4: Also at Federal University of Rio Grande do Sul, Porto Alegre, Brazil
5: Also at Université Libre de Bruxelles, Bruxelles, Belgium
6: Also at Institute for Theoretical and Experimental Physics, Moscow, Russia
7: Also at Joint Institute for Nuclear Research, Dubna, Russia
8: Also at Zewail City of Science and Technology, Zewail, Egypt
9: Now at Fayoum University, El-Fayoum, Egypt
10: Also at British University in Egypt, Cairo, Egypt
11: Now at Ain Shams University, Cairo, Egypt
12: Also at Department of Physics; King Abdulaziz University, Jeddah, Saudi Arabia
13: Also at Université de Haute Alsace, Mulhouse, France
14: Also at Skobeltsyn Institute of Nuclear Physics; Lomonosov Moscow State University, Moscow, Russia
15: Also at CERN; European Organization for Nuclear Research, Geneva, Switzerland
16: Also at RWTH Aachen University; III. Physikalisches Institut A, Aachen, Germany
17: Also at University of Hamburg, Hamburg, Germany
18: Also at Brandenburg University of Technology, Cottbus, Germany
19: Also at MTA-ELTE Lendület CMS Particle and Nuclear Physics Group; Eötvös Loránd University, Budapest, Hungary
20: Also at Institute of Nuclear Research ATOMKI, Debrecen, Hungary
21: Also at Institute of Physics; University of Debrecen, Debrecen, Hungary
22: Also at Indian Institute of Technology Bhubaneswar, Bhubaneswar, India
23: Also at Institute of Physics, Bhubaneswar, India
24: Also at Shoolini University, Solan, India
25: Also at University of Visva-Bharati, Santiniketan, India
26: Also at University of Ruhuna, Matara, Sri Lanka
27: Also at Isfahan University of Technology, Isfahan, Iran
28: Also at Yazd University, Yazd, Iran
29: Also at Plasma Physics Research Center; Science and Research Branch; Islamic Azad University, Tehran, Iran
30: Also at Università degli Studi di Siena, Siena, Italy
31: Also at INFN Sezione di Milano-Bicocca; Università di Milano-Bicocca, Milano, Italy
32: Also at Purdue University, West Lafayette, USA
33: Also at International Islamic University of Malaysia, Kuala Lumpur, Malaysia
34: Also at Malaysian Nuclear Agency; MOSTI, Kajang, Malaysia
35: Also at Consejo Nacional de Ciencia y Tecnología, Mexico city, Mexico
36: Also at Warsaw University of Technology; Institute of Electronic Systems, Warsaw, Poland
37: Also at Institute for Nuclear Research, Moscow, Russia
38: Now at National Research Nuclear University 'Moscow Engineering Physics Institute' (MEPhI), Moscow, Russia
39: Also at St. Petersburg State Polytechnical University, St. Petersburg, Russia
40: Also at University of Florida, Gainesville, USA

41: Also at P.N. Lebedev Physical Institute, Moscow, Russia
42: Also at California Institute of Technology, Pasadena, USA
43: Also at Budker Institute of Nuclear Physics, Novosibirsk, Russia
44: Also at Faculty of Physics; University of Belgrade, Belgrade, Serbia
45: Also at University of Belgrade; Faculty of Physics and Vinca Institute of Nuclear Sciences, Belgrade, Serbia
46: Also at Scuola Normale e Sezione dell'INFN, Pisa, Italy
47: Also at National and Kapodistrian University of Athens, Athens, Greece
48: Also at Riga Technical University, Riga, Latvia
49: Also at Universität Zürich, Zurich, Switzerland
50: Also at Stefan Meyer Institute for Subatomic Physics (SMI), Vienna, Austria
51: Also at Adiyaman University, Adiyaman, Turkey
52: Also at Istanbul Aydin University, Istanbul, Turkey
53: Also at Mersin University, Mersin, Turkey
54: Also at Piri Reis University, Istanbul, Turkey
55: Also at Gaziosmanpasa University, Tokat, Turkey
56: Also at Izmir Institute of Technology, Izmir, Turkey
57: Also at Necmettin Erbakan University, Konya, Turkey
58: Also at Marmara University, Istanbul, Turkey
59: Also at Kafkas University, Kars, Turkey
60: Also at Istanbul Bilgi University, Istanbul, Turkey
61: Also at Rutherford Appleton Laboratory, Didcot, United Kingdom
62: Also at School of Physics and Astronomy; University of Southampton, Southampton, United Kingdom
63: Also at Monash University; Faculty of Science, Clayton, Australia
64: Also at Instituto de Astrofísica de Canarias, La Laguna, Spain
65: Also at Utah Valley University, Orem, USA
66: Also at Beykent University, Istanbul, Turkey
67: Also at Bingol University, Bingol, Turkey
68: Also at Erzincan University, Erzincan, Turkey
69: Also at Sinop University, Sinop, Turkey
70: Also at Mimar Sinan University; Istanbul, Istanbul, Turkey
71: Also at Texas A&M University at Qatar, Doha, Qatar
72: Also at Kyungpook National University, Daegu, Korea